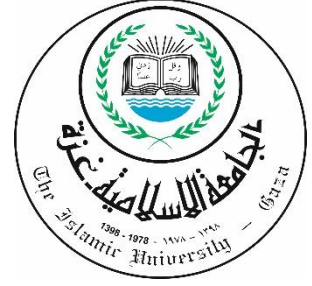


**Islamic University-Gaza
Research and Graduate Studies Affairs
Faculty of Engineering
Electrical Engineering Department
Communication Systems Engineering**



Reconfigurable Phased Array Patch Antenna for Ku-Band Satellite Communication Systems

تصميم مصفوفة هوائيات الشرائح الرقيقة لأنظمة اتصالات الأقمار الصناعية على نطاق Ku

Prepared By:

Moahmmmed Awny Matar

Supervisors:

Dr. Talal F. Skaik

**A thesis Submitted in Partial Fulfillment of the requirements for
the Degree of Master in Electrical Engineering –
Communication Systems Engineering**

2016 - 1437



نتيجة الحكم على أطروحة ماجستير

بناءً على موافقة شئون البحث العلمي والدراسات العليا بالجامعة الإسلامية بغزة على تشكيل لجنة الحكم على أطروحة الباحث/ محمد عوني إبراهيم مطر لنيل درجة الماجستير في كلية الهندسة قسم الهندسة الكهربائية - أنظمة الاتصالات وموضوعها:

تصميم مصفوفة هوائيات الشرائح الرقيقة لأنظمة اتصالات الأقمار الصناعية على نطاق ku
Reconfigurable Phased Array Patch Antenna for Ku-band Satellite
Communication Systems

وبعد المناقشة التي تمت اليوم الأربعاء 30 جمادى الآخر 1437هـ، الموافق 2016/03/30 الساعة العاشرة والنصف صباحاً، اجتمعت لجنة الحكم على الأطروحة والمكونة من:

.....	مشرفاً و رئيساً	د. طلال فايز سكيك
..... Ammar	مناقشاً داخلياً	د. عمار محمد رمضان/ أبو هدروس
.....	مناقشاً خارجياً	د. مصطفى حسن أبو نصر

وبعد المداولة أوصت اللجنة بمنح الباحث درجة الماجستير في كلية الهندسة/ قسم الهندسة الكهربائية -

أنظمة الاتصالات.

واللجنة إذ تمنحه هذه الدرجة فإنها توصيه بتقوى الله ولزوم طاعته وأن يسخر علمه في خدمة دينه ووطنه.

والله والتوفيق،،،

نائب الرئيس لشئون البحث العلمي والدراسات العليا

أ.د. عبدالرؤوف علي المناعمة



نموذج رقم (1)

إقرار

أنا الموقع أدناه مقدم الرسالة التي تحمل العنوان:

Reconfigurable Phased Array Patch Antenna for Ku-band Satellite Communication Systems

أقر بأن ما اشتملت عليه هذه الرسالة إنما هو نتاج جهدي الخاص، باستثناء ما تمت الإشارة إليه
حيثما ورد، وإن هذه الرسالة ككل أو أي جزء منها لم يقدم من قبل لنيل درجة أو لقب علمي أو
بحثي لدى أي مؤسسة تعليمية أو بحثية أخرى.

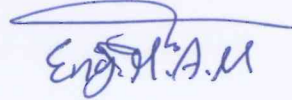
DECLARATION

The work provided in this thesis, unless otherwise referenced, is the
researcher's own work, and has not been submitted elsewhere for any
other degree or qualification

Student's name:

اسم الطالب: محمد عوني ابراهيم مطر

Signature:

التوقيع: 

Date:

التاريخ: 20/4/2016

To the most beloved people in my life

My parents: Awny and Samia

My sisters and brothers

My wife: Asmaa

My grandparents

Contents

List of figures	VI
List of tables	IX
Abstract	X
1. Introduction	1
1.1 Phased array antenna	1
1.1.1 Array background	1
1.2 Advanced Design System (ADS).....	2
1.3 Varactor Diode	3
1.4 Satellite Communication	4
1.3.1 Frequency Allocations for Satellite Services	4
1.3.2 The Earth Segment.....	6
1.5 Literature Review	8
1.6 Thesis Motivation.....	9
1.6.1 Thesis Contribution	9
1.7 Thesis Overview.....	9
2. Antenna Theory	11
2.1 Introduction	11
2.2 Maxwell's Equations.....	12
2.3 Antenna Parameters.....	14
2.3.1 Introduction.....	14
2.3.2 Radiation Pattern.....	14
2.3.3 Radiation Power Density	15
2.3.4 Radiation Intensity	16
2.3.5 Beamwidth	17
2.3.6 Directivity	18
2.3.7 Antenna Efficiency and Gain.....	18
2.3.8 Bandwidth.....	20
2.3.9 Polarization	20
2.4 Microstrip Patch Antennas	21

2.4.1	Introduction.....	21
2.4.2	Technical Background	22
2.4.3	Feed/Excitation Methods	24
2.4.4	Rectangular Patch	26
2.4.5	Transmission-Line Model.....	27
2.4.6	Input Impedance.....	31
2.5	Conclusion.....	32
3.	Phased Antenna Array	33
3.1	Introduction	33
3.2	Array Theory	33
3.3	Planar Array	36
3.4	Antenna Beamforming	38
3.4.1	Analog Beam Forming.....	38
3.4.2	Digital Beam Forming	40
3.5	Means of Phase Shifting.....	41
3.5.1	Phase Shifting by Changing Frequency	42
3.5.2	Phase Shifting by Changing Length	43
3.5.3	Phase Shifting by Changing Permittivity.....	44
3.5.4	Phase Shifting by Changing Permeability	44
3.6	Phased Array Architecture	46
3.6.1	Phased Arrays based on feed network design.....	46
3.6.2	Phased array based on phase shift stage	48
3.6.3	Primary and secondary array	51
3.7	Conclusion.....	51
4.	Design and Implementation.....	52
4.1	Introduction	52
4.2	IF Circuit Design	54
4.3	Phase Shifters Design.....	55
4.4	Antenna design.....	59
4.4.1	Design L-band antenna	59
4.4.2	Beam Steering with enhanced gain phased array antenna	64

4.4.3	Design of Ku-band antenna	67
4.5	4-Element Array Design.....	69
4.6	Simulation of the whole system	70
4.7	Conclusion.....	71
5.	Conclusion and future work	72
5.1	Performance Comparison.....	72
5.2	Future Work	74
Appendix A	75
6.	References.....	80

List of figures

Figure 1.1 Phased array antenna system [3]	1
Figure 1.2 Advanced Design System (ADS)	3
Figure 1.3 The usage of varicap in microwave phase shifters	3
Figure 1.4 Communication Satellite Links	4
Figure 1.5 Block diagram showing a home terminal for DBS TV/FM reception [6]	7
Figure 1.6 Thesis Structure	10
Figure 2.1 1887 experimental set-up of Hertz's apparatus [2]	11
Figure 2.2 wave propagation [5]	14
Figure 2.3 Coordinate system for antenna analysis [4].	15
Figure 2.4 Three- and two-dimensional power patterns (in linear scale) [4]	17
Figure 2.5 means of S11 bandwidth	20
Figure 2.6 Polarization ellipse [4]	21
Figure 2.7 Components of a Patch Antenna (Feed Not Shown) [19]	22
Figure 2.8 Two different capacitive feed methods for relatively thick substrates [8].	24
Figure 2.9 Tear-drop and cylindrical-shaped feed probes for relatively thick substrates [20].	25
Figure 2.10 Configuration of microstrip patch elements [20].	25
Figure 2.11 Non-contact proximity feed from underneath the patch [20].	26
Figure 2.12 Non-contact proximity feed from edge of patch [20].	27
Figure 2.13 Patch fed by aperture-coupling slot [20].	27
Figure 2.14 Microstrip line feed [4].	28
Figure 2.15 Microstrip line and its electric field lines, and effective dielectric constant geometry [4].	29
Figure 2.16 Physical and effective lengths of rectangular microstrip patch [4].	30
Figure 2.17 Typical variation of resistance and reactance of rectangular microstrip antenna [4].	32
Figure 3.1 Geometry of two-element array separated by a distance d [37].	34
Figure 3.2 Far-field geometry of two dipoles [37].	34

Figure 3.3 Geometrical configuration of N isotropic elements along the z-axis, separated by a distance d and fed with a progressive phase ξ [37]	35
Figure 3.4 Geometry of a rectangular M \times N planar array with interelement distance d [37].	37
Figure 3.5 Architecture of a simple, on-beam RF beam former [37].	38
Figure 3.6(a) A Butler beam-forming matrix for a four-element antenna array, and (b) its phasing scheme [37].	39
Figure 3.7 Computation of the antenna pattern corresponding to the beam former in Figure 3.6 [46]	40
Figure 3.8 Simple digital beam-former architecture [37].	41
Figure 3.9 Series-fed linear array antenna consisting of K identical elements, equidistantly displaced d with respect to one another [49].	42
Figure 3.10 Phase shifters in a linear phased array antenna feed network. a, b. Series-fed linear phased array antenna. c. Corporate-fed linear phased array antenna [49].	43
Figure 3.11 Cascaded, four-bit, digitally switched phase shifter [49].	44
Figure 3.12 Basic Reggia–Spencer phase shifter configuration [49].	45
Figure 3.13 Single section (bit) of a latched ferrite phase shifter [49].	45
Figure 3.14 General diagram of parallel fed phased array [2].	46
Figure 3.15 General diagram of series fed phased array [2]	47
Figure 3.16 General diagram of RF phase shifting phased array [2].	48
Figure 3.17 General diagram of LO phase shifting phased array [2].	49
Figure 3.18 General diagram of IF phase shifting phased array [2]	50
Figure 3.19 Grouping antennas into a sub array each using one phase shifter can reduce the number of required phase shifters [2]	51
Figure 4.1 The conventional design of phased arrays requires one phase shifter for each antenna element [2].	52
Figure 4.2 In hybrid couplers phased array, phase shifters and power dividing network are combined in a single entity	52
Figure 4.3 The IF distribution network at 1.7 GHz	54
Figure 4.4 Phases between the antennas element	54
Figure 4.5 IF Phase shifter	55
Figure 4.6 Phase shifter insertion loss	56

Figure 4.7 Phase shifts with varying the capacitance	56
Figure 4.8 BB833 varactor Capacitance versus applied voltage	57
Figure 4.9 Scattering parameters simulation results.....	58
Figure 4.10 Phase shift between adjacent ports	58
Figure 4.11 The initial phase progression across the IF ports	59
Figure 4.12 L-Band Antenna Dimensions	60
Figure 4.13 2D Radiation Pattern of L-Band Antenna	60
Figure 4.14 Return Loss of L-Band Antenna.....	61
Figure 4.15 Beamforming array at L-band domain	61
Figure 4.16 Radiation pattern when $C=1.5$ pF	62
Figure 4.17 Radiation pattern when $C=0.001$ pF	62
Figure 4.18 Radiation pattern when $C=4.5$ pF	63
Figure 4.19 Radiation pattern when $C=3$ pF	63
Figure 4.20 Radiation pattern when $C=0.5$ pF	64
Figure 4.21 Two elements array L-band antenna.....	65
Figure 4.22 Beamforming circuit with L-band subarrays	66
Figure 4.23 Radiation pattern of new phased array when (a) $C=0.001$ pf, (b) $C=1.5$ pf.....	66
Figure 4.24 Radiation pattern of new phased array when (a) $C=3$ pf, (b) $C=4.5$	67
Figure 4.25 Ku-band Antenna dimensions	67
Figure 4.26 2D Radiation Pattern of Ku-band antenna	68
Figure 4.27 Ku-band Antenna return loss.....	68
Figure 4.28 Ku-band Array antenna dimensions	69
Figure 4.29 2D radiation pattern of Ku-band array.....	70
Figure 4.30 Array Antenna return loss (S_{11}).....	70
Figure 4.31 Ku-band steering system	71

List of tables

Table 1.1 Frequency Band Designations [3]	6
Table 2.1 Generalized Forms of Maxwell's Equations [16]	12
Table 5.1 Comparison between the series-fed phased array presented in this chapter and the published series-fed phased arrays	73

Abstract

Phased array antenna technology is emerging as new way to deal with the growing demand for more powerful, cost effective and highly efficient wireless systems. This thesis presents phased array antenna at Ku-band for satellite system applications with steering capability to receive signals from different satellites. The proposed feeding structure consists of hybrid couplers and phase shifters in order to distribute the power and achieve the desired phase shift using varactors. The feeding network is series-fed circuit connected to an array of microstrip patch antennas, and it performs phase shifting in the intermediate frequency IF stage. The simulation is done using Advanced Design System (ADS) 2014 software. The simulation results show that a scanning range of 50 degrees has been achieved with gain variation of 1.3 dB.

ملخص البحث

قام الباحثون بتطوير تقنية مصفوفة هوائيات الشرائح الرقيقة كأداة جديدة للتعامل مع الطلب المتزايد على أنظمة اتصالات لاسلكية تتمتع بكفاءة عمل عالية. هذه الرسالة تقدم مصفوفة هوائيات شرائح دقيقة تعمل في نطاق (Ku) لتطبيقات اتصالات الأقمار الصناعية قادرة على تغيير زاوية استقبال الإشارة للتعامل مع أقمار صناعية في أماكن مختلفة. تتكون دائرة التغذية المقترحة في هذا النظام من دوائر تعمل على توزيع وتأخير الإشارة المدخلة بالمقدار المطلوب من خلال مكثفات متغير السعة حتى نحصل على زاوية الاستقبال المطلوبة. دائرة التوزيع في هذا النظام متسلسلة التغذية متصلة بمصفوفة هوائيات رقيقة تعمل على توزيع وتأخير الإشارة في نطاق التردد المتوسط (IF). تمت محاكاة النظام المصمم باستخدام برنامج ADS 2014. المحاكاة أظهرت زاوية مسح تقدر وصلت 50 درجة مع تغير في الكسب وصل الى 1.3 dB .

1. Introduction

In this thesis, phased array patch antenna in Ku-band is presented. This antenna is designed to receive the Ku-band signal from different locations electronically without any mechanically movement. In this chapter, general background about the arrays and its applications is introduced.

1.1 Phased array antenna

Several antennas can be arranged in space and interconnected to produce a directional radiation pattern. Such a configuration of multiple radiating elements is referred to as an array antenna, or simply, an array [1]. Phased array antenna is a multiple-antenna system in which the radiation pattern can be reinforced in a particular direction and suppressed in undesired directions as shown in Figure 1.1. The direction of phased array radiation can be electronically steered obviating the need for any mechanical rotation. These unique capabilities have found phased arrays a broad range of applications since the advent of this technology [2]. One of these applications is Satellite communication systems.

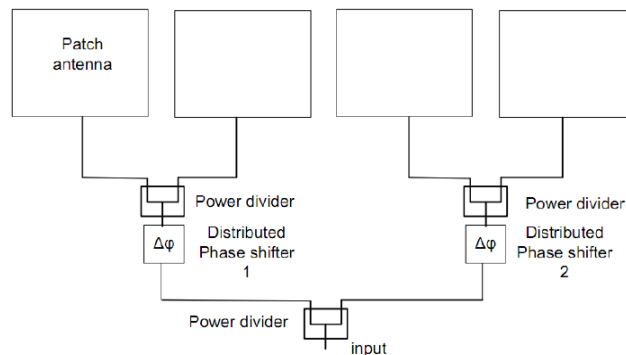


Figure 1.1 Phased array antenna system [3]

1.1.1 Array background

Usually the radiation pattern of a single element is relatively wide, and each element provides low values of directivity (gain). In many applications it is necessary to design antennas with very directive characteristics (very high gains) to meet the demands of long distance communication. This can only be accomplished by increasing the electrical size of the antenna. Enlarging the dimensions of single elements often leads to more directive characteristics. Another way to enlarge

the dimensions of the antenna, without necessarily increasing the size of the individual elements, is to form an assembly of radiating elements in an electrical and geometrical configuration. This new antenna, formed by multi-elements, is referred to as an *array*. In most cases, the elements of an array are identical. This is not necessary, but it is often convenient, simpler, and more practical. The individual elements of an array may be of any form (wires, apertures, etc.). The total field of the array is determined by the vector addition of the fields radiated by the individual elements. This assumes that the current in each element is the same as that of the isolated element (neglecting coupling). This is usually not the case and depends on the separation between the elements. To provide very directive patterns, it is necessary that the fields from the elements of the array interfere constructively (add) in the desired directions and interfere destructively (cancel each other) in the remaining space. Ideally this can be accomplished, but practically it is only approached. In an array of identical elements, there are at least five controls that can be used to shape the overall pattern of the antenna [4].

These are:

1. The geometrical configuration of the overall array (linear, circular, rectangular, spherical, etc.)
2. The relative displacement between the elements.
3. The excitation amplitude of the individual elements.
4. The excitation phase of the individual elements.
5. The relative pattern of the individual elements.

1.2 Advanced Design System (ADS)

Advanced Design System (ADS) software is “the world’s leading electronic design automation (EDA) software for Radio Frequency (RF), microwave and high speed digital applications” [5].

ADS is a simulator like spice, cadence. But it focuses on the RF and microwave design, so most of its devices on the library are microwave devices. In designing the microwave filters and antennas, ADS provides a powerful and easy-to-use interfaces. For wireless and radars applications, ADS provides full, standered-based design and varification with Wirless Librareies and circuit-system-EM co-simulation in an integrated platform [5].



Figure 1.2 Advanced Design System (ADS)

1.3 Varactor Diode

In electronics, a varicap diode, varactor diode, variable capacitance diode, variable reactance diode or tuning diode is a type of diode whose capacitance varies as a function of the voltage applied across its terminals. Varactors are used as voltage controlled capacitors. They are commonly used in voltage-controlled oscillators, phase shifters, and frequency multipliers. Voltage-controlled oscillators have many applications such as frequency modulation for FM transmitters and phase-locked loops. The varicap was developed by the Pacific Semiconductor subsidiary of the Ramo Wooldridge Corporation who received a patent for the device in June 1961 [2]. The device name was also trademarked as the "Varicap", the successor to Pacific Semiconductors, in October 1967. Figure 1.3 illustrate one of the applications that use varicap in microwave phase shifters.

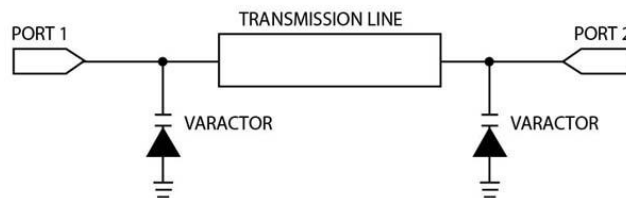


Figure 1.3 The usage of varicap in microwave phase shifters

1.4 Satellite Communication

The use of satellites in communication systems is very much a fact of everyday life, as is evidenced by the many homes equipped with antennas, or “dishes,” used for reception of satellite television. What may not be so well known is that satellites form an essential part of telecommunications systems worldwide, carrying large amounts of data and telephone traffic in addition to television signals. Satellites offer a number of features not readily available with other means of communications. Because very large areas of the earth are visible from a satellite, the satellite can form the star point of a communications net, simultaneously linking many users who may be widely separated geographically. The same feature enables satellites to provide communications links to remote communities in sparsely populated areas that are difficult to access by other means. Of course, satellite signals ignore political boundaries as well as geographic ones, which may or may not be a desirable feature. Satellites are also used for remote sensing, examples being the detection of water pollution and the monitoring and reporting of weather conditions. Some of these remote sensing satellites also form a vital link in search and rescue operations for downed aircraft and the like.

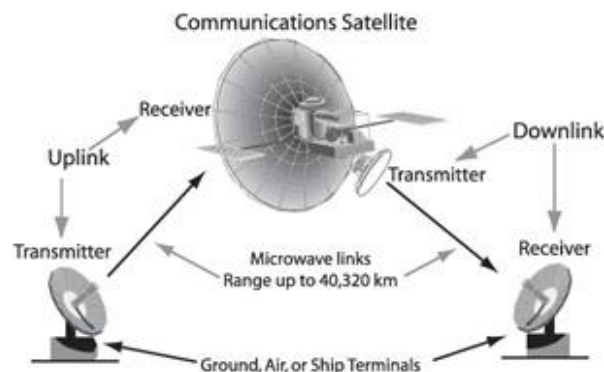


Figure 1.4 Communication Satellite Links

1.3.1 Frequency Allocations for Satellite Services

Allocating frequencies to satellite services is a complicated process which requires international coordination and planning. This is carried out under the auspices of the International Telecommunication Union (ITU). To facilitate frequency planning, the world is divided into three regions:

Region 1: Europe, Africa, what was formerly the Soviet Union, and Mongolia

Region 2: North and South America and Greenland

Region 3: Asia (excluding region 1 areas), Australia, and the southwest Pacific

Within these regions, frequency bands are allocated to various satellite services, although a given service may be allocated different frequency bands in different regions. Some of the services provided by satellites are: *Fixed satellite service (FSS)*, *Broadcasting satellite service (BSS)*, *Mobile satellite services*, *Navigational satellite services*, *Meteorological satellite services*.

There are many subdivisions within these broad classifications; for example, the FSS provides links for existing telephone networks as well as for transmitting television signals to cable companies for distribution over cable systems. Broadcasting satellite services are intended mainly for direct broadcast to the home, sometimes referred to as direct broadcast satellite (DBS) service [in Europe it may be known as direct-to-home (DTH) service]. Mobile satellite services would include land mobile, maritime mobile, and aeronautical mobile. Navigational satellite services include global positioning systems (GPS), and satellites intended for the meteorological services often provide a search and rescue service [6]. Table 1.1 lists the frequency band designations in common use for satellite services. The Ku band signifies the band under the K band, and the Ka band is the band above the K band. The Ku band is the one used at present for DBS, and it is also used for certain FSS. The C band is used for FSS, and no DBS is allowed in this band. The very high frequency (VHF) band is used for certain mobile and navigational services and for data transfer from weather satellites. The L band is used for mobile satellite services and navigation systems. For the FSS in the C band, the most widely used subrange is approximately 4 to 6 GHz. The higher frequency is nearly always used for the uplink to the satellite; common practice is to denote the C band by 6/4 GHz, giving the uplink frequency first. For the direct broadcast service in the Ku band, the most widely used range is approximately 12 to 14 GHz, which is denoted by 14/12 GHz. Although frequency assignments are made much more precisely, and they may lie somewhat outside the values quoted here (an example of assigned frequencies in the Ku band is 14,030 and 11,730 MHz), the approximate values stated are quite satisfactory for use in calculations involving frequency [6].

Table 1.1 Frequency Band Designations [3]

Frequency range, (GHz)	Band designation
0.1-0.3	VHF
0.3-1.0	UHF
1.0-2.0	L
2.0-4.0	S
4.0-8.0	C
8.0-12.0	X
12.0-18.0	Ku
18.0-27.0	K
27.0-40.0	Ka
40.0-75	V
75-110	W
110-300	mm
300-3000	μm

1.3.2 The Earth Segment

The earth segment of a satellite communications system consists of the transmit and receive earth stations. The simplest of these are the home *TV receive-only* (TVRO) systems, and the most complex are the terminal stations used for international communications networks. Also included in the earth segment are those stations which are on ships at sea, and commercial and military land and aeronautical mobile stations. In Receive-Only Home TV Systems, Planned broadcasting directly to home TV receivers takes place in the Ku (12-GHz) band. This service is known as direct broadcast satellite (DBS) service. There is some variation in the frequency bands assigned to different geographic regions. In the Americas, for example, the downlink band is 12.2 to 12.7 GHz. Figure 1.5 shows the main units in a home terminal DBS TV receiving system.

Although there will be variations from system to system, the diagram covers the basic concept for analog [*frequency modulated* (FM)] TV [6].

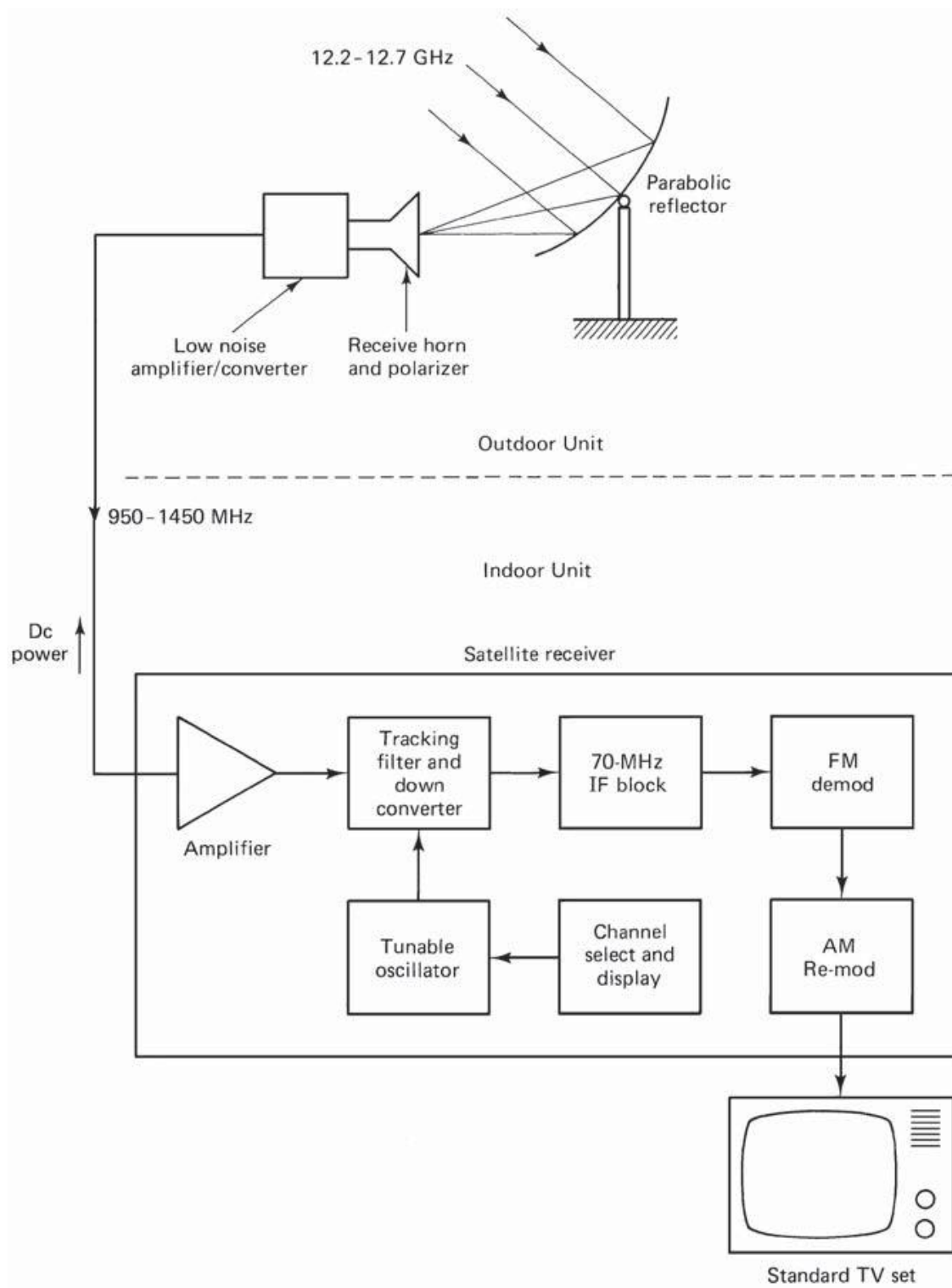


Figure 1.5 Block diagram showing a home terminal for DBS TV/FM reception [6]

1.5 Literature Review

Phased array technology for satellite communication applications is an increasingly interesting and growing commercial market for satellite terminals, so that there are a lot of researches in this field. Here, some researches which are related to our project will be presented. In [2], three new approaches to the design of phased array antennas are presented in order to reduce their complexity. The first approach is based on extended resonance technique and the second one is based on a bi-directional feeding method. Finally, the third approach allows the phase progression across the antenna elements to be controlled by using a single phase shifter. In [7], prototype of an electronically steerable receives-only array antenna realized within the ESA-project NATALIA is presented. The antenna is conceived for the reception of mobile satellite services in Ku-band and its design targets the market of automotive applications. The design of the prototype is based on an innovative polarization agile phased array concept and exhibits an excellent RF-performance as well as a very compact envelope. In [8], the authors present a new phased array antenna design capable of mechanical scanning in azimuth and electronic scanning in elevation. Non-resonant slot coupled patch antenna with a parasitic element on top is designed for wideband operation, which covers entire Ku band allocated for TV reception, and high gain. In [9], an S-band phased array was designed for communication between satellite in geostationary orbit and a spacecraft in Lower Earth Orbit (LEO). The array was designed for left-hand circular polarization (LHCP) since many satellite applications use circular polarization to avoid alignment problems while orbiting earth. In [10], the paper presents a field measurement of a simple antenna system mounted on a vehicle by utilizing a geostationary test satellite called Engineering Test Satellite VIII (ETS-VIII). The developed antenna system is compact, lightweight, and promising for low-cost production. The antenna system is constructed by a 16-cm patch array antenna, which has simple satellite tracking that is controlled by a control unit as the vehicle's bearing is updated from a navigation system in real time. In [11], a Ku-band, electronically-steerable, Artificial-impedance-Surface Antenna (AISA) was designed, fabricated and measured. It is capable of scanning in elevation from -70 to 80° with gain variation of less than 5 dB. In [12], the article presents the design of a low cost fully active phased array antenna with specific emphasis on the realization of an elementary radiating cell. The phased array antenna is designed for mobile satellite services and dedicated for automotive applications. In [13], the authors discuss the problem of applying reflector antenna on

moving vehicle, and present a low profile phased array antenna as a solution for such problem. The fabrication of the low profile phased array antenna is analyzed, and then the elevation pattern of the antenna is optimized by Genetic Algorithm (GA). The elevation pattern of the antenna with initial sub-array distances and optimized sub-array distances are contrasted, and the sub-array distances by GA optimization are obtained.

1.6 Thesis Motivation

Television transmission directly to home receivers has been one of the more successful commercial applications of satellite communications. This lead many researchers to develop an equipment that make the usage of this application easier. The common receiving antenna used for reception is large-size reflector that occupy large space and require a motor for mechanical steering to receive from different satellites. This research aims to develop a microwave receiving alternative antenna based on Microstrip planner technology with an array of patch antennas. The size of the planner system is smaller than of the reflector. Moreover, electronic steering is another interest in the current research to capture TV signals from different satellite without the need to move the physical receiving antenna.

1.6.1 Thesis Contribution

In this thesis, antenna beam steering technique will be presented as a solution of receiving TV channels from satellites which stand in various locations in the space. This will be achieved without any mechanical movement of the receiving antenna like the conventional dishes, but with electronic steering to enable the designed antenna from receiving TV channels from both Nilesat and Arabsat satellites.

1.7 Thesis Overview

The structure of the thesis is illustrated in Figure 1.6. In more detail, Chapter 2 provides an overview of the theory of Antenna. The work in chapter 2 presents the antenna parameters which describe the behavior of antenna and its limitations in the overall efficiency. Later in the same chapter, Microstrip patch antenna and its design considerations is presented. In chapter 3, Phased array antenna is described. Antenna beamforming and the microwave phase shifters will be presented. Chapter 4 is the core of this thesis, and it present the design and implementation of

reconfigurable phased array antenna. The last chapter present the conclusion drawn from the current work and also future work.

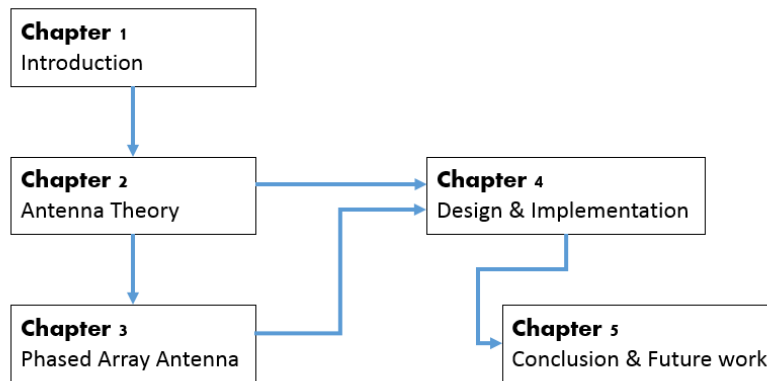


Figure 1.6 Thesis Structure

2. Antenna Theory

2.1 Introduction

Webster's Dictionary defines the antenna as "a usually metallic device (as a rod or wire) for radiating or receiving radio waves." The IEEE Standard Definitions of Terms for defines the antenna or aerial as "a means for radiating or receiving radio waves." We can say that the antenna is the transitional device between free-space and a guiding lines [4]. Work on antennas started many years ago. The first antenna experiment was done by the German physicist Heinrich Rudolf Hertz (1857–1894). The SI (International Standard) frequency unit, the Hertz, is named after him. In 1887 he built a system, as shown in Figure 2.1, to generate and detect radio waves. The original aim of his experiment was to prove the existence of electromagnetic radiation [14]. Whilst Heinrich Hertz performed his experiments in a laboratory and did not quite know what radio waves might be used for in practice, Guglielmo Marconi (1874–1937), an Italian inventor, developed and commercialized wireless technology by introducing a radiotelegraph system, which served as the foundation for the establishment of numerous affiliated companies worldwide. His most famous experiment was the transatlantic transmission from Poldhu, UK to St Johns, Newfoundland in Canada in 1901, employing untuned systems [14].

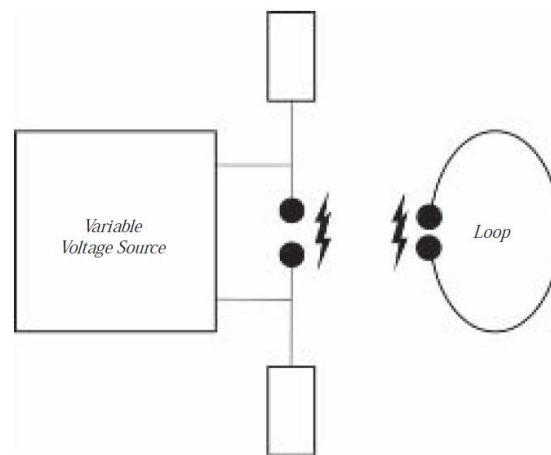


Figure 2.1 1887 experimental set-up of Hertz's apparatus [2]

Since Hertz and Marconi, antennas have become increasingly important to our society until now they are indispensable. They are everywhere; at our homes and workplaces, on our cars and

aircraft, while our ships, satellites and spacecraft bristle with them. Even as pedestrian, we carry them [15]. This chapter provides theoretical background about the electromagnetic waves and its propagation in space. Maxwell's Equations will be presented in order to understand the reality of electromagnetic waves. In section three, the radiation device "Antenna" will take place by presenting its parameters. Section four will present the Microstrip patch antenna as a type of antenna that will be designed in the current work and will be presented in later chapters.

2.2 Maxwell's Equations

The Scottish James Clerk Maxwell (1831-1879) is regarded as the founder of electromagnetic theory in its present form. Maxwell's famous work led to the discovery of electromagnetic waves. Through his theoretical efforts when he was between 35 and 40 years old, Maxwell published the first unified theory of electricity and magnetism. The theory involved all previously known results, both experimental and theoretical, on electricity and magnetism. It further introduced displacement current and predicted the existence of electromagnetic waves. Maxwell's equations were not accepted by many scientists until 1888, when they were confirmed by Heinrich Rudolf Hertz. The generalized forms of Maxwell's equations are shown in Table 2.1 [16].

Table 2.1 Generalized Forms of Maxwell's Equations [16]

Differential Form	Integral Form	Remarks
$\nabla \cdot \mathbf{D} = \rho_v$	$\oint_S \mathbf{D} \cdot d\mathbf{S} = \int_v \rho_v dv$	Gauss's law
$\nabla \cdot \mathbf{B} = 0$	$\oint_S \mathbf{B} \cdot d\mathbf{S} = 0$	Nonexistence of isolated magnetic charge
$\nabla \times \mathbf{E} = -\frac{\partial \mathbf{B}}{\partial t}$	$\oint_L \mathbf{E} \cdot d\mathbf{l} = -\frac{\partial}{\partial t} \oint_S \mathbf{B} \cdot d\mathbf{S}$	Faraday's law
$\nabla \times \mathbf{H} = \mathbf{J} + \frac{\partial \mathbf{D}}{\partial t}$	$\oint_L \mathbf{H} \cdot d\mathbf{l} = \int_S \left(\mathbf{J} + \frac{\partial \mathbf{D}}{\partial t} \right) \cdot d\mathbf{S}$	Ampere's circuit law

The first and the second are Gauss' laws for the electric and magnetic fields, the third is Faraday's law of induction, the fourth is Ampere's law as amended by Maxwell to include $\partial\mathbf{D}/\partial t$. The displacement current term $\partial\mathbf{D}/\partial t$ in Ampere's law is essential in predicting the existence of propagating electromagnetic waves. Its role in establishing charge conservation. The equations in table 2.1 are in SI units. The quantities \mathbf{E} and \mathbf{H} are the electric and magnetic field intensities and are measured in units of [volt/m] and [ampere/m], respectively. The quantities \mathbf{D} and \mathbf{B} are the electric and magnetic flux densities and are in units of [coulomb/m²] and [weber/m²], or [tesla]. \mathbf{D} is also called electric displacement, and \mathbf{B} , the magnetic induction. The quantities ρ and \mathbf{J} are the volume charge density and electric current density (charge flux) of any external charge (that is, not including any induced polarization charges and currents.). They are measured in units of [coulomb/m³] and [ampere/m²]. The right-hand side of the second equation is zero because there are no magnetic monopole charges. The charge and current densities ρ and \mathbf{J} may be thought of as the source of electromagnetic fields. For wave propagation problems, these densities are localized in space; for example, they are restricted to flow on an antenna. The generated electric and magnetic fields are radiated away from these sources and can propagate to large distance to the receiving antennas. Away from the sources, that is, in source-free regions of space, Maxwell's equations take the simpler form [17]:

$$\nabla \times \mathbf{E} = -\frac{\partial \mathbf{B}}{\partial t}$$

$$\nabla \times \mathbf{H} = \frac{\partial \mathbf{D}}{\partial t}$$

$$\nabla \cdot \mathbf{D} = 0$$

(Source-free Maxwell's equations)

2.1

$$\nabla \cdot \mathbf{B} = 0$$

The qualitative mechanism by which Maxwell's equations give rise to propagating electromagnetic fields is shown in the figure below. For example, a time-varying current $I(t)$ on a linear antenna generates a circulating and time-varying magnetic field \mathbf{H} , which through Faraday's law generates a circulating electric field \mathbf{E} , which through Ampere's law generates a magnetic field, and so on. The cross-linked electric and magnetic fields propagate away from the current source [17].

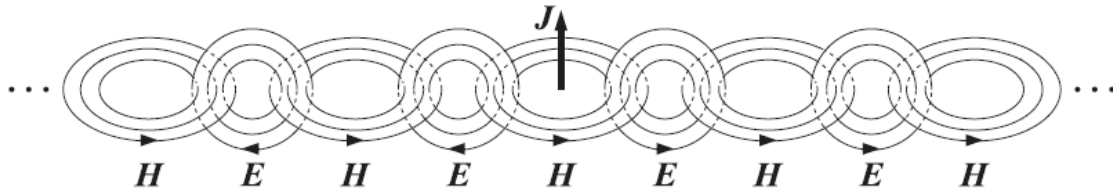


Figure 2.2 wave propagation [5]

2.3 Antenna Parameters

2.3.1 Introduction

To describe the performance of an antenna, definitions of various parameters are necessary. Some of the parameters are related with each other and not all of them need be specified for complete description of the antenna performance [4].

2.3.2 Radiation Pattern

An antenna *radiation pattern* or *antenna pattern* is defined as “a mathematical function or a graphical representation of the radiation properties of the antenna as a function of space coordinates. In most cases, the radiation pattern is determined in the far field region and is represented as a function of the directional coordinates. Radiation properties include power flux density, radiation intensity, field strength, directivity, phase or polarization.” The radiation property of most concern is the two- or three dimensional spatial distribution of radiated energy as a function of the observer’s position along a path or surface of constant radius. A convenient set of coordinates is shown in Figure 2.3. A trace of the received electric (magnetic) field at a constant radius is called the amplitude field *pattern*. On the other hand, amplitude *power pattern* is defined as a graph of the spatial variation of the power density along a constant radius. Often the *field* and *power* patterns are normalized with respect to their maximum value, yielding *normalized field* and *power patterns*. The power pattern is usually plotted on a logarithmic scale or more commonly in decibels (dB). This scale is usually desirable because a logarithmic scale can stand out in more details those parts of the pattern that have very low values [4].

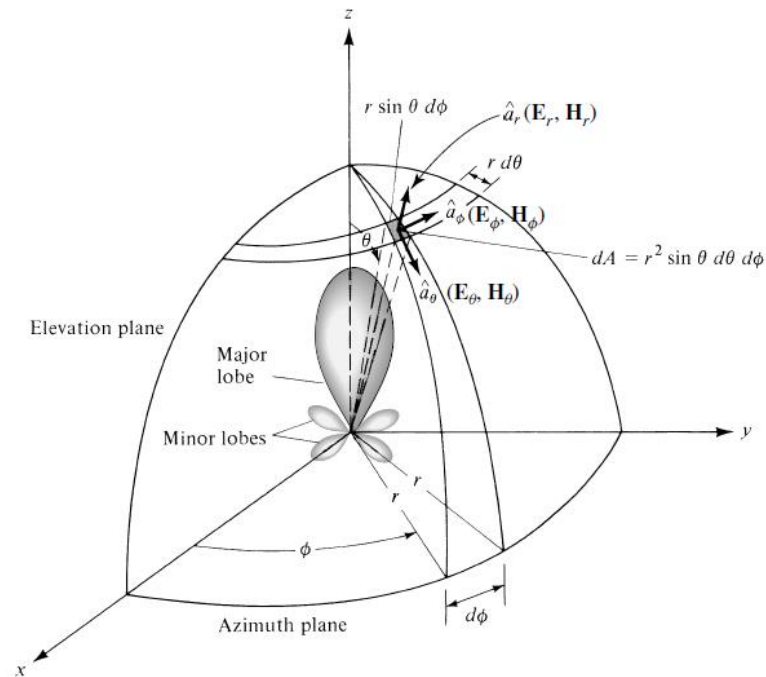


Figure 2.3 Coordinate system for antenna analysis [4].

For an antenna, the

- Field pattern (in linear scale)* represents a plot of the magnitude of the electric or magnetic field as a function of the angular space.
- Power pattern (in linear scale)* represents a plot of the square of the magnitude of the electric or magnetic field as a function of the angular space.
- Power pattern (in dB)* represents the magnitude of the electric or magnetic field, in decibels, as a function of the angular space [4].

2.3.3 Radiation Power Density

Instantaneous Poynting vector is a quantity which used to describe the power associated with an electromagnetic wave and defined as [4]

$$\mathbf{W} = \mathbf{E} \times \mathbf{H} \quad 2.2$$

\mathbf{W} = instantaneous Poynting vector (W/m²)

\mathbf{E} = instantaneous electric-field intensity (V/m)

\mathbf{H} = instantaneous magnetic-field intensity (A/m)

Since the Poynting vector is a power density, the total power crossing a closed surface can be obtained by integrating the normal component of the Poynting vector over the entire surface. In equation form [4]

$$P = \oint_S \mathbf{W} \cdot d\mathbf{S} = \oint_S \mathbf{W} \cdot \bar{\mathbf{n}} da \quad 2.3$$

P = instantaneous total power (W)

$\bar{\mathbf{n}}$ = unit vector normal to the surface

da = infinitesimal area of the closed surface (m^2)

For time-varying fields applications, it is often more desirable to find the average power density which is obtained by integrating the instantaneous Poynting vector over one period and dividing by the period [4]

$$\mathbf{W}_{av}(x, y, z) = [W(x, y, z; t)]_{av} = \frac{1}{2} \text{Re}[\mathbf{E} \times \mathbf{H}^*] \quad 2.4$$

Based upon the previous equation, the average power radiated by an antenna (radiated power) can be written as [4]

$$\begin{aligned} P_{rad} = P_{av} &= \oint_S \mathbf{W}_{rad} \cdot d\mathbf{S} = \oint_S \mathbf{W}_{av} \cdot \bar{\mathbf{n}} da \\ &= \frac{1}{2} \oint_S \text{Re}[\mathbf{E} \times \mathbf{H}^*] \cdot d\mathbf{S} \end{aligned} \quad 2.5$$

2.3.4 Radiation Intensity

Steradian is the measure unit of solid angle. One *steradian* is defined as the solid angle with its vertex at the center of a sphere of radius r that is subtended by a spherical surface area equal to that of a square with each side of length r . Since the area of a sphere of radius r is $A = 4\pi r^2$, there are 4π sr ($4\pi r^2/r^2$) in a closed sphere. *Radiation intensity* in a given direction is “the power radiated from an antenna per unit solid angle.” The radiation intensity can be obtained by simply multiplying the radiation density by the square of the distance. In mathematical form it is expressed as [4]

$$U = r^2 W_{rad} \quad 2.6$$

U = radiation intensity (W/unit solid angle)

W_{rad} = radiation density (W/m^2)

The total power is obtained by integrating the radiation intensity, as given by (2.6), over the entire solid angle of 4π . Thus [4]

$$P_{rad} = \oint_{\Omega} U d\Omega = \int_0^\pi \int_0^{2\pi} U \sin\theta d\theta d\phi \quad 2.7$$

Where $d\Omega$ = element of solid angle = $\sin\theta d\theta d\phi$

2.3.5 Beamwidth

The beamwidth of an antenna is a very important figure of merit and often is used as a trade-off between it and the side lobe level; that is, as the beamwidth decreases, the side lobe increases and vice versa. In addition, the beamwidth of the antenna is also used to describe the resolution capabilities of the antenna to distinguish between two adjacent radiating sources or radar targets. *Half-Power Beamwidth (HPBW)* is one of the most widely used beamwidths, which is defined by IEEE as: “In a plane containing the direction of the maximum of a beam, the angle between the two directions in which the radiation intensity is one-half value of the beam.” Another important beamwidth is First-Null Beamwidth (FNBW) which is the angular separation between the first nulls of the pattern. Both the HPBW and FNBW are demonstrated for the pattern in Figure 2.4 [4].

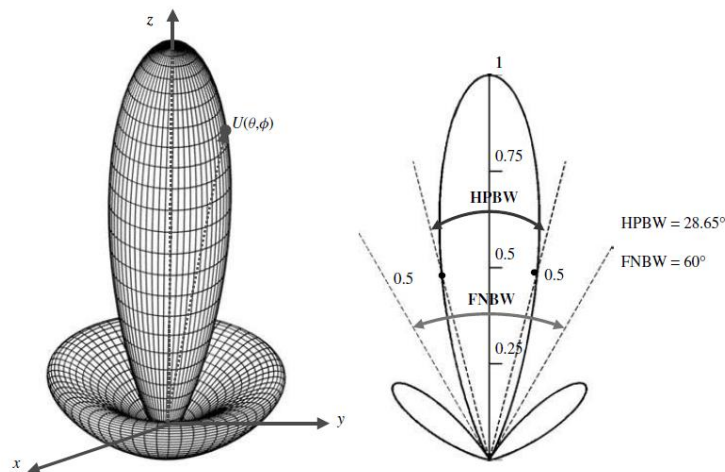


Figure 2.4 Three- and two-dimensional power patterns (in linear scale) [4]

2.3.6 Directivity

Directivity is defined as the ratio of the radiation intensity in a given direction from the antenna to the radiation intensity averaged over all directions. The average radiation intensity is equal to the total power radiated by the antenna divided by 4π . Simply, the directivity of a nonisotropic source is equal to the ratio of its radiation intensity in a given direction over that of an isotropic source. In mathematical form, using (2.8), it can be written as [4]

$$\mathbf{D} = \mathbf{D}(\theta, \phi) = \frac{U(\theta, \phi)}{U_0} = \frac{4\pi U(\theta, \phi)}{P_{rad}} \quad 2.8$$

If the direction is not specified, the direction of maximum radiation intensity is implied [4].

$$\mathbf{D}_{max} = \mathbf{D}_0 = \frac{U}{U_0} = \frac{U_{max}}{U_0} = \frac{4\pi U_{max}}{P_{rad}} \quad 2.9$$

Where:

\mathbf{D} = directivity (dimensionless)

\mathbf{D}_0 = maximum directivity (dimensionless)

$U = U(\theta, \phi)$ = radiation intensity (W/S_r)

U_{max} = maximum radiation intensity (W/S_r)

U_0 = radiation intensity of isotropic source (W/S_r)

P_{rad} = total radiated power (W)

2.3.7 Antenna Efficiency and Gain

The total antenna efficiency e_0 is used to take into account losses at the input terminals and within the structure of the antenna. In general, the overall efficiency can be written as [4]

$$e_0 = e_r e_c e_d \quad 2.10$$

Where

e_0 = total efficiency (dimensionless)

e_r = reflection (mismatch) efficiency = $(1 - |\Gamma|^2)$ (dimensionless)

e_c = conduction efficiency (dimensionless)

e_d = dielectric efficiency (dimensionless)

$$\Gamma = \frac{Z_{in} - Z_0}{Z_{in} + Z_0}$$

$$\text{VSWR} = \text{voltage standing wave ratio} = \frac{1+|\Gamma|}{1-|\Gamma|}$$

Γ = voltage reflection coefficient at the input terminals of the antenna

Z_{in} = antenna input impedance

Z_0 = characteristic impedance of the transmission line.

Usually e_c and e_d are very difficult to compute, but they can be determined experimentally. It is usually more convenient to write (2.10) as

$$e_0 = e_r e_{dc} = e_{cd}(1 - |\Gamma|^2), \quad 2.11$$

where $e_{dc} = e_c e_d$ = antenna radiation efficiency, which is used to relate the gain and directivity.

The Gain of the antenna is closely related to the directivity. In addition to the directional capabilities it account the efficiency of the antenna. Gain does not account for losses arising from impedance mismatches (reflection losses) and polarization mismatches (losses). Gain is the ratio of the intensity, in gain direction, to the radiation intensity that would be obtained if the power accepted by the antenna were radiated isotropically [4].

$$\text{Gain} = 4\pi \frac{\text{radiation intensity}}{\text{total input accepted power}} = 4\pi \frac{U(\theta, \phi)}{P_{in}} \quad (\text{dimensionless}) \quad 2.12$$

We can write that the total radiated power (P_{rad}) is related to the total input power (P_{in}) by

$$P_{rad} = e_{cd} P_{in} \quad 2.13$$

$$G(\theta, \phi) = e_{cd} \left[4\pi \frac{U(\theta, \phi)}{P_{rad}} \right] \quad 2.14$$

$$G(\theta, \phi) = e_{cd} D(\theta, \phi) \quad 2.15$$

The maximum value of the gain is related to the maximum directivity

$$G_0 = e_{cd} D_0 \quad 2.16$$

2.3.8 Bandwidth

For broadband antennas, the bandwidth is usually expressed as the ratio of the upper-to-lower frequencies of the acceptable operation which is -10 dB in return loss. For example, a 10:1 bandwidth indicates that the upper frequency is 10 times greater than the lower. For narrowband antennas, the bandwidth is expressed as a percentage of the frequency difference (upper minus lower) over the center frequency of the bandwidth. For example For example, a 5% bandwidth indicates that the frequency difference of acceptable operation is 5% of the center frequency of the bandwidth [4].The figure below presents the -10dB and -6 dB bandwidth for given antenna.

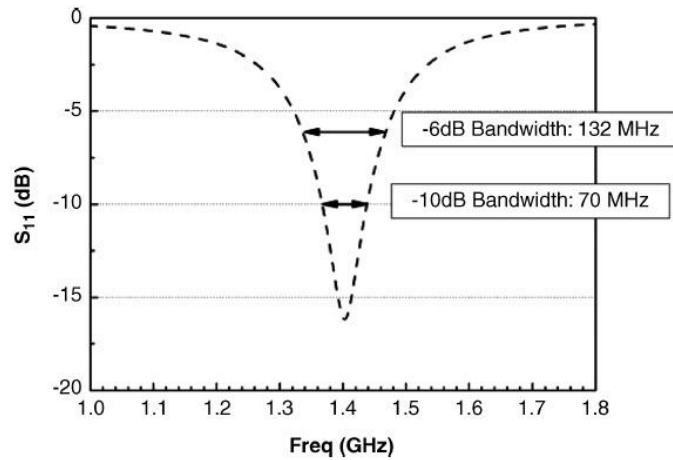


Figure 2.5 means of S11 bandwidth

2.3.9 Polarization

Polarization is defined as “the curve traced by the end point of the arrow (vector) representing the instantaneous electric field” [4]. The field must be observed along the direction of propagation. Polarization is classified into three types linear, circular, or elliptical. If the vector that describes the electric field at a point in space as a function of time is always directed along a line, the field is said to be linearly polarized. Linear polarization and circular polarization are special cases of elliptic polarization. Polarization can be clockwise (CW, right-hand polarization), or counter clockwise (CCW, left-hand polarization) [18]. The instantaneous electric field of a plane wave, traveling in the negative z direction, can be written as [4]

$$E(z; t) = \mathbf{a}_x E_x(z; t) + \mathbf{a}_y E_y(z; t) \quad 2.17$$

By considering the complex counterpart of these instantaneous components, we can write

$$E_x(z; t) = E_{x0} \cos(\omega t + kz + \phi_x) \quad 2.18$$

$$E_y(z; t) = E_{y0} \cos(\omega t + kz + \phi_y) \quad 2.19$$

Where E_{x0} and E_{y0} are the maximum magnitudes of the x- and y-components as seen in Figure 2.6, ω is the angular frequency, kz is the direction component, ϕ_x and ϕ_y is the phase shifts [18].

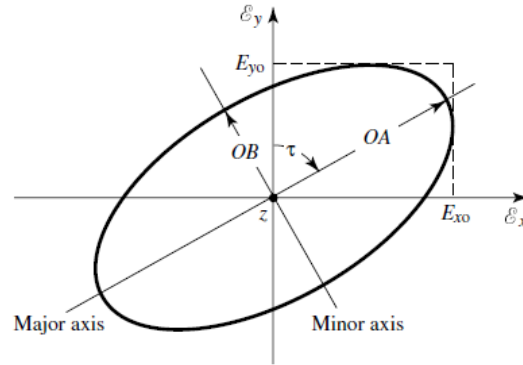


Figure 2.6 Polarization ellipse [4]

2.4 Microstrip Patch Antennas

2.4.1 Introduction

A radiating element with the attractive characteristic that it has a low profile is the *patch antenna*, illustrated in Figure 2.7. It consists of a thin metallic film above a grounded dielectric substrate, and has the additional advantages of being lightweight, conformable, economical to manufacture, and easily connected to solid state devices [19]. The results of these properties share in to the success of microstrip antennas not only in military applications such as aircraft, missiles, rockets, and spacecraft but also in commercial areas such as mobile satellite communications, terrestrial cellular communications, direct broadcast satellite (DBS) system, global positioning system (GPS), remote sensing, and hyperthermia [20]. The patch can be any shape, but the regular geometric shapes (such as rectangles or circular discs) are most commonly used [19].

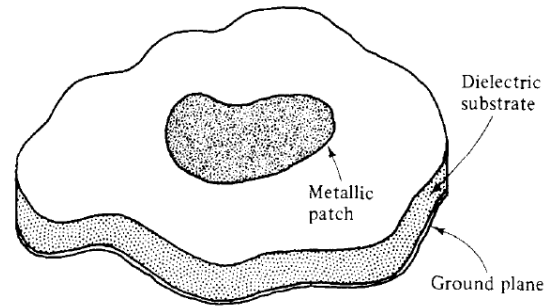


Figure 2.7 Components of a Patch Antenna (Feed Not Shown) [19]

2.4.2 Technical Background

This sub-section presents the technical background of the microstrip patch antenna, which is separated into three areas: features of the microstrip antenna, advantage and disadvantage trade-offs, and material considerations.

a. Features of the Microstrip Antenna

At the early stage of its development, the microstrip antenna [21] [22], as shown in Figure 2.7, is generally a single-layer design and consists of a radiating conductive patch or an array of patches situated on one side of a thin, non-conducting, substrate panel with a metallic ground plane situated on the other side of the panel. The metallic patch is normally made of thin copper foil or is copper-foil plated with a corrosion resistive metal, such as gold, tin, or nickel. There are many shapes of patch antenna, the most popular shapes are rectangular or circular. The substrate generally has a thickness in the range of 0.01–0.05 free-space wavelength (λ_0). It is used primarily to provide proper spacing and mechanical support between the patch and its ground plane. It is also often used with high dielectric-constant material to load the patch and reduce its size. The substrate material should be low in insertion loss with a loss tangent of less than 0.005, in particular, for large array application. Generally, substrate materials [22] can be separated into three categories in accordance with their dielectric constant [20]:

1. Having a relative dielectric constant (ϵ_r) in the range of 1.0–2.0. This type of material can be air, polystyrene foam, or dielectric honeycomb.
2. Having ϵ_r in the range of 2.0–4.0 with material consisting mostly of fiberglass reinforced Teflon.
3. With an ϵ_r between 4 and 10. The material can consist of ceramic, quartz, or alumina.

Although there are materials with ϵ_r much higher than 10, one should be careful in using these materials. As to be discussed later, they can significantly reduce the antenna's radiation efficiency.

b. Advantage and Disadvantage Trade-offs

There are advantages as well as disadvantages associated with the microstrip antenna. By understanding them well, one can readily design a microstrip antenna with optimum efficiency, minimum risk, and lower cost for a particular application. The advantages of microstrip antennas when compared to conventional antennas (helix, horn, reflector, etc.) are the following [20].

1. The extremely low profile of the microstrip antenna makes it lightweight and it occupies very little volume of the structure or vehicle on which it is mounted [23] [24].
2. The patch element or an array of patch elements, when produced in large quantities, can be fabricated with a simple etching process, which can lead to greatly reduced fabrication cost. The patch element can also be integrated or made monolithic with other microwave active/passive components [20].
3. Multiple-frequency operation is possible by using either stacked patches or a patch with loaded pin or a stub [25].

The disadvantages of the microstrip antennas are the following

1. A single-patch microstrip antenna with a thin substrate (thickness less than 0.02 free-space wavelength) generally has a narrow bandwidth of less than 5% [20].
2. The microstrip antenna can handle relatively lower RF power due to the small separation between the radiating patch and its ground plane (equivalent to small separation between two electrodes) [20].
3. The microstrip array generally has a larger ohmic insertion loss than other types of antennas of equivalent aperture size. This ohmic loss mostly occurs in the dielectric substrate and the metal conductor of the microstrip line power dividing circuit. It should be noted that a single-patch element generally incurs very little loss because it is only one-half wavelength long [22].

2.4.3 Feed/Excitation Methods

A microstrip patch antenna can be fed or excited to radiate by many techniques; several common ones are listed and briefly discussed next.

a. Coax Probe Feed

Thicker substrate is generally used for wider bandwidth (5–15%) applications. If we use a regular coax probe, a larger inductance would be introduced, which results in impedance mismatch. We can say that, the electrical field confined in the small cylindrical space of the coax cannot suddenly transition into the large spacing of the patch. To cancel the inductance occurring at the feed, capacitive reactance must be introduced. One method to solve this problem is to use a capacitive disk [26] as shown in Figure 2.8 where the patch is not physically connected to the probe. Another method is to use a “tear-drop” shaped [27] or a cylindrical shaped probe [28] as illustrated in Figure 2.9. With this method the probe is soldered to the patch, where mechanical rigidity may be offered for some applications.

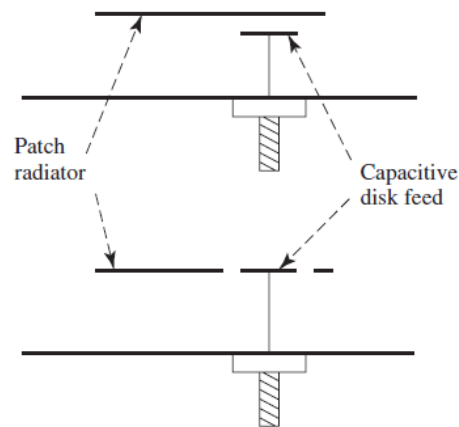


Figure 2.8 Two different capacitive feed methods for relatively thick substrates [8].

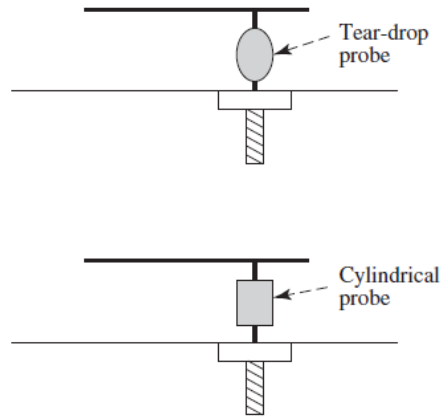


Figure 2.9 Tear-drop and cylindrical-shaped feed probes for relatively thick substrates [20].

b. Microstrip-Line Feed

Figure 2.10 illustrated that a microstrip patch antenna can be connected directly to a microstrip transmission line. At the edge of a patch, impedance is generally much higher than 50 ohms (e.g., 200 ohms). To avoid impedance mismatch, sections of quarter-wavelength long impedance transformers [29] can be used to transform a large input impedance to a 50-ohm line.

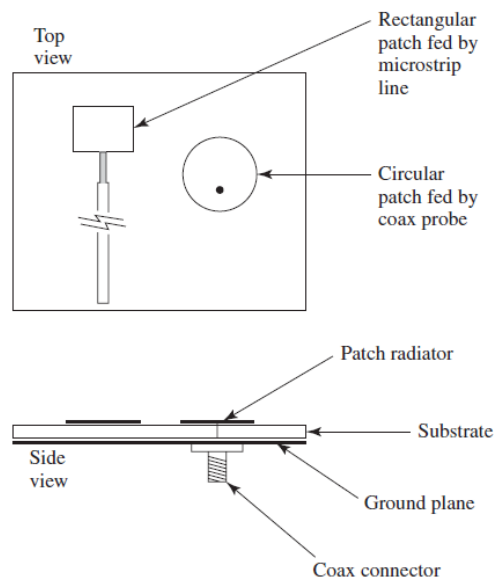


Figure 2.10 Configuration of microstrip patch elements [20].

c. Proximity-Coupled Microstrip Line Feed

An open-ended microstrip feeding line can be used to excite a patch antenna through proximity coupling. For example, the open end of a 100-ohm line can be placed underneath the patch antenna at its 100-ohm location as shown in Figure 2.11. The open-ended microstrip line can also be placed in parallel and very close to the edge of patch, as shown in Figure 2.12, to achieve feeding through fringe-field coupling [30]. Both these methods will help to avoid any soldering connection, which in some cases could achieve better mechanical reliability.

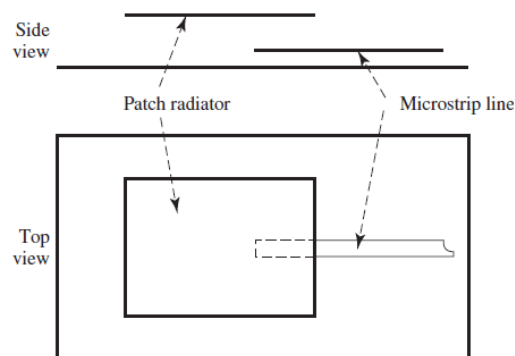


Figure 2.11 Non-contact proximity feed from underneath the patch [20].

d. Aperture-Coupled Feed

An open-ended microstrip feeding line or stripline transmission line can be placed on one side of the ground plane to excite the patch antenna situated on the other side through an opening slot in the ground plane. This slot-coupling or aperture-coupling technique [31], as shown in Figure 2.13, can be used to avoid a soldering connection, as well as to avoid leakage radiation of the lines that interferes with the patch radiation. In addition, this feed method generally allows the patch antenna to have wider bandwidth ($>10\%$) with a thick substrate or extremely wide bandwidth ($>30\%$) with stacked parasitic patches.

2.4.4 Rectangular Patch

The rectangular patch antenna is the most widely used configuration. It is very easy to analyze using both the transmission-line and cavity models, which are most accurate for thin substrates [32]. We will present the transmission-line model because it is easier to illustrate.

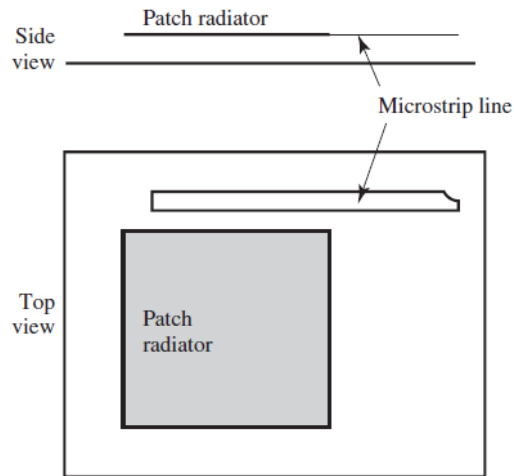


Figure 2.12 Non-contact proximity feed from edge of patch [20].

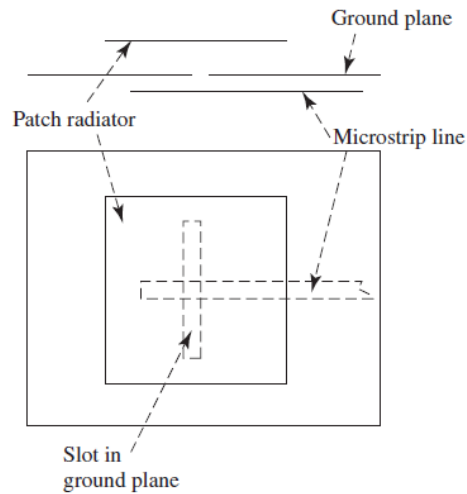


Figure 2.13 Patch fed by aperture-coupling slot [20].

2.4.5 Transmission-Line Model

It was indicated earlier that the transmission-line model is the easiest of all but it yields the least accurate results and it lacks the versatility. However, it does shed some physical insight. Basically the transmission-line model represents the microstrip antenna by two slots, separated by a low-impedance Z_c transmission line of length L [4].

A. Fringing Effects

The dimensions of the patch are finite along the length and width, so the fields at the edges of the patch undergo fringing. This is illustrated along the length in Figure 2.14 for the two radiating slots of the microstrip antenna. The same applies along the width. The amount of fringing is a function of the dimensions of the patch and the height of the substrate (h). For the principal E -plane (xy -plane) fringing is a function of the ratio of the length of the patch L to the height h of the substrate (L/h) and the dielectric constant ϵ_r of the substrate. Since for microstrip antennas $L/h \gg 1$, fringing is reduced; however, it must be taken into account because it has an impact on the resonant frequency of the antenna. The same applies for the width [4].

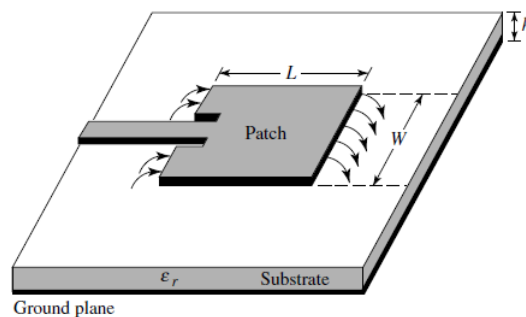


Figure 2.14 Microstrip line feed [4].

For a microstrip line shown in Figure 2.15(a), typical electric field lines are shown in Figure 2.15 (b). This is a nonhomogeneous line of two dielectrics; the substrate and air. As we can see, most of the electric field lines are inside the substrate and parts of some lines exist in air. As $W/h \gg 1$ and $\epsilon_r \gg 1$, the electric field lines concentrate mostly in the substrate. Fringing in this case makes the microstrip line look wider electrically compared to its physical dimensions. Since some of the waves travel in the substrate and some in air, an *effective dielectric constant* $\epsilon_{r\text{eff}}$ is introduced to account for fringing and the wave propagation in the line [4].

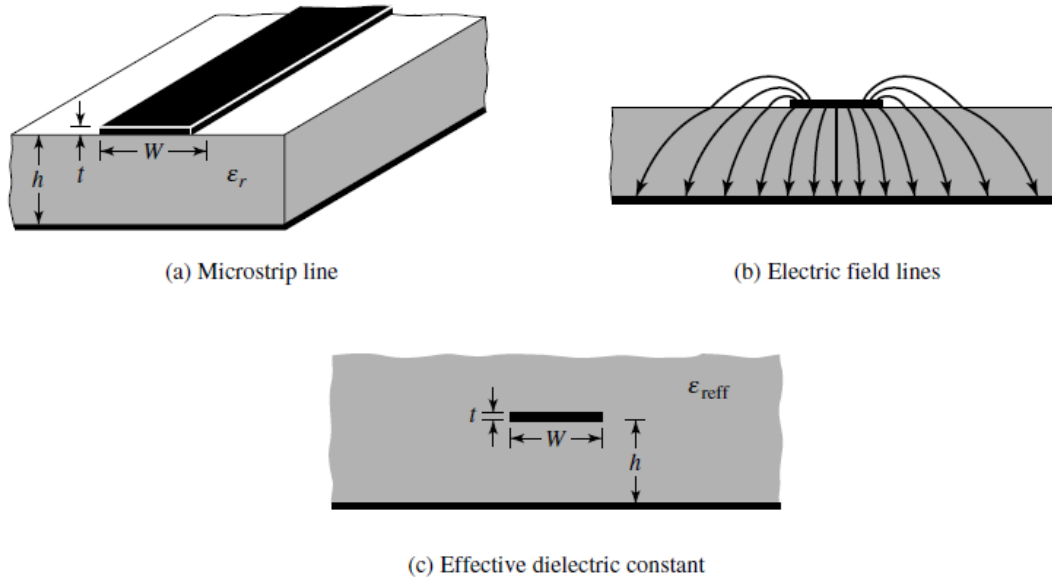


Figure 2.15 Microstrip line and its electric field lines, and effective dielectric constant geometry [4].

To introduce the effective dielectric constant, let us assume that the center conductor of the microstrip line with its original dimensions and height above the ground plane is embedded into one dielectric, as shown in Figure 2.15(c). The effective dielectric constant is defined as “the dielectric constant of the uniform dielectric material so that the line of Figure 2.15(c) has identical electrical characteristics, particularly propagation constant, as the actual line of Figure 2.15(a)” [4]. The effective dielectric constant is also a function of frequency. As the frequency of operation increases, most of the electric field lines concentrate in the substrate. Therefore the microstrip line behaves more like a homogeneous line of one dielectric (only the substrate), and the effective dielectric constant approaches the value of the dielectric constant of the substrate [4]. The initial values (at low frequencies) of the effective dielectric constant are referred to as the *static values*, and they are given by [33]

$$\epsilon_{reff} = \frac{\epsilon_r + 1}{2} + \frac{\epsilon_r - 1}{2} \left[1 + 12 \frac{h}{w} \right]^{-1/2} \quad W/h > 1 \quad 2.20$$

B. Effective Length, Resonant Frequency, and Effective Width

Because of the fringing effects, the patch of the patch microstrip antenna looks electrically greater than its physical dimensions. For the principal *E*-plane (*xy*-plane), this is demonstrated in

Figure 2.16 where the dimensions of the patch along its length have been extended on each end by a distance ΔL , which is a function of the effective dielectric constant ϵ_{reff} and the width-to-height ratio (W/h) [4]. A very popular and practical approximate relation for the normalized extension of the length is [34]

$$\frac{\Delta L}{h} = 0.412 \frac{(\epsilon_{reff} + 0.3) \left(\frac{W}{h} + 0.264 \right)}{(\epsilon_{reff} - 0.258) \left(\frac{W}{h} + 0.8 \right)} \quad 2.21$$

Since the length of the patch has been extended by ΔL on each side, the effective length of the patch is now [4]

$$L_{eff} = L + 2\Delta L \quad 2.22$$

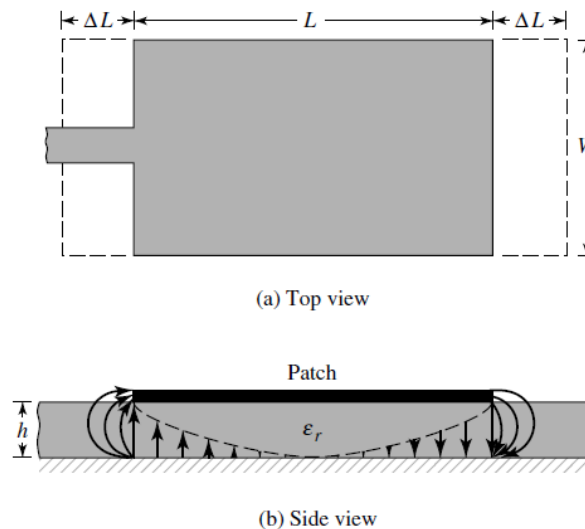


Figure 2.16 Physical and effective lengths of rectangular microstrip patch [4].

C. Design

We assume that the specified information includes the dielectric constant of the substrate (ϵ_r), the resonant frequency (f_r), and the height of the substrate h are known. The procedure is as follows:

Specify:

ϵ_r , f_r (in Hz), and h

Determine:

W , L

Design procedure:

1. For an efficient radiator, a practical width that leads to good radiation efficiencies is [35]

$$W = \frac{1}{2f_r\sqrt{\mu_0\epsilon_0}} \sqrt{\frac{2}{\epsilon_r+1}} = \frac{v_0}{2f_r} \sqrt{\frac{2}{\epsilon_r+1}}, \quad 2.23$$

where, v_0 is the free-space velocity of light.

2. Determine the effective dielectric constant of the microstrip patch antenna using (2.20).
3. Once W is determined using (2.23), find the extension of the length ΔL using (2.21).
4. Now, the actual length of the patch can be determined for L .

$$L = \frac{1}{2f_r\sqrt{\epsilon_{reff}}\sqrt{\mu_0\epsilon_0}} - 2\Delta L \quad 2.24$$

2.4.6 Input Impedance

The input impedance is complex and it includes both a resonant and a non-resonant part which is usually reactive. Both the real and imaginary parts of the impedance change as a function of frequency, and a typical variation is shown in Figure 2.17. Ideally both the resistance and reactance exhibit symmetry about the resonant frequency, and the reactance at resonance is equal to the average of sum of its maximum value (which is positive) and its minimum value (which is negative). Typically the feed reactance is very small, compared to the resonant resistance, for very thin substrates. However, for thick elements the reactance may be significant and needs to be taken into account in impedance matching and in determining the resonant frequency of a loaded element [36].

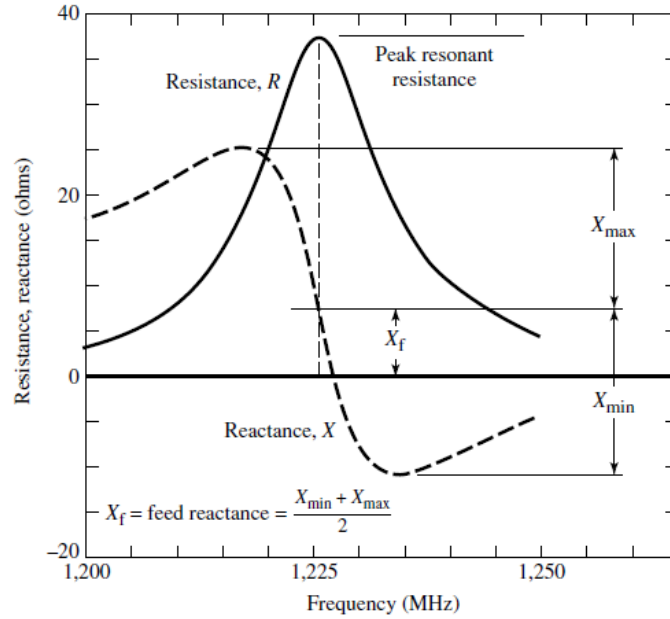


Figure 2.17 Typical variation of resistance and reactance of rectangular microstrip antenna [4].

2.5 Conclusion

In this chapter, we present the theoretical image about the antenna and its parameters. Maxwell's equations were introduced in section 2.2 as the concept of wave propagation. In section 2.4 Microstrip patch antenna was presented based on the previous sections and this section will be the base of the later chapters. In next chapter, phased antenna and beamforming theory will be presented as the core of design chapter.

3. Phased Antenna Array

3.1 Introduction

Arrays are geometrical configurations of multiple antennas arranged in space, in order to yield highly directive patterns. In an array antenna, the fields from the individual elements add constructively in some directions and destructively (cancel) in others. For analysis, arrays are assumed to consist of identical elements, although it is possible to create an array with elements such that each has a different radiation pattern [37]. The major advantage of antenna arrays over a single antenna element is their electronic scanning capability. In scanning, the major lobe can be steered toward any direction by changing the relative phase of the excitation current at each array element (phased array antennas). Furthermore, by also controlling the magnitude of the excitation current, a large variety of radiation patterns and sidelobe level characteristics can be produced. Adaptive antennas (also called “smart antennas” in mobile communication applications) go a step further than phased arrays and can direct their main lobe (with increased gain) in a desired direction (e.g., a mobile user in a cellular communication system) and nulls in the directions of interference or jammers. There are five main parameters that affect the overall performance of an antenna array [38]:

1. Geometry (e.g., linear, circular, or planar arrangement of the radiating elements)
2. Distance of separation between adjacent elements
3. Amplitude current excitation of each individual element
4. Phase excitation of each individual element
5. Radiation pattern of each individual element

3.2 Array Theory

Firstly, let us assume an antenna array with two infinitesimal horizontal dipoles in free space, positioned as shown in Figure 3.1. The first dipole is located at $(0, 0, d/2)$ and carries a current of $I_0 \angle (\xi/2)$ and the other one at $(0, 0, -d/2)$ with current $I_0 \angle (\xi/2)$, where ξ is the phase difference added to the two dipoles externally through a phase shifter.

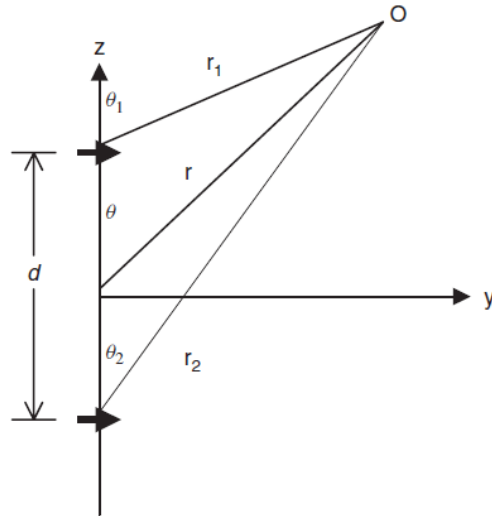


Figure 3.1 Geometry of two-element array separated by a distance d [37].

The total electric field at the test point O is given as the vector summation of the fields due to the two individual antennas [38] (without considering mutual coupling effects):

$$E_{total} = E_1 + E_2 = \widehat{a}_\theta \frac{j\eta k l_0}{4\pi} l \left(\frac{e^{-j(kr_1 - \xi/2)}}{r_1} |\cos \theta_1| + \frac{e^{-j(kr_2 + \xi/2)}}{r_2} |\cos \theta_2| \right) \quad 3.1$$

where, η is the intrinsic impedance of the medium, and $k^2 = \omega^2 \mu \epsilon$, r_1 and r_2 are the distances between the antennas and the observation point. In the far field r_1, r_2 and r are parallel as shown in Figure 3.2, so $\theta_1 \approx \theta_2 \approx \theta$ and $r_1 \approx r_2 \approx r$ for amplitude variations and $r_1 \approx r - (d/2) \cos \theta$ and $r_2 \approx r + (d/2) \cos \theta$ for phase variations. Hence equation (3.1) can be rewritten as follow [37]

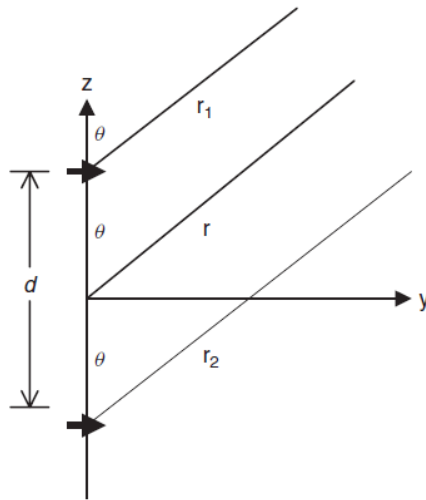


Figure 3.2 Far-field geometry of two dipoles [37].

$$E_{total} = E_1 + E_2 = \widehat{a}_\theta \frac{j\eta k l_0}{4\pi r} l e^{-jkr} |\cos \theta| 2 \cos \left[\frac{1}{2} (kd \cos \theta + \xi) \right] \quad 3.2$$

Looking at equations (3.1) and (3.2) one can observe that the total field is equal to the field of the single element (*element factor*) located at the origin, multiplied by an *array factor* (AF) given by

$$AF = 2 \cos \left[\frac{1}{2} (kd \cos \theta + \xi) \right] \quad 3.3$$

Generally, the far-field pattern of an array is given by the *multiplication pattern* of the single element and the array factor:

$$Total\ Pattern = Element\ Factor \times Array\ Factor \quad 3.4$$

The array factor is a function of the following parameters [37]:

1. The geometrical arrangement of the radiating elements comprising the array
2. The current excitation of the elements
3. The number of elements
4. The distance of separation d of adjacent elements
5. Frequency (or wavelength) of operation

Consider now an N -element array of isotropic radiators shown in Figure 3.3. Since all elements of the array are positioned along a single line, it is called a linear array and it is uniform because each identical element is fed with a current of the same magnitude but with a progressive phase shift of ξ . The distance of separation between adjacent elements is d .

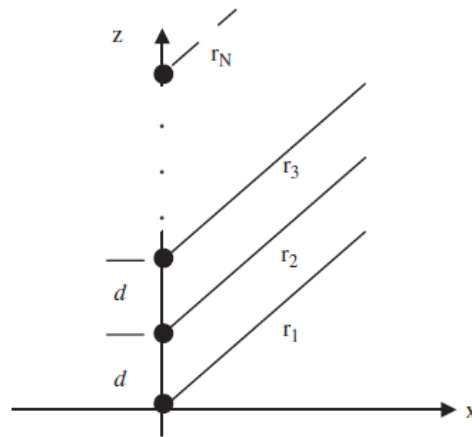


Figure 3.3 Geometrical configuration of N isotropic elements along the z -axis, separated by a distance d and fed with a progressive phase ξ [37].

In this case the array factor can be expressed as the sum of all single-element contributions:

$$AF = 1 + e^{j\psi} + e^{j2\psi} + e^{j3\psi} + \dots + e^{j(N-1)\psi} \quad 3.5$$

Where $\psi = kd \cos \theta + \xi$. Equation (3.5) is a geometric series that can be expressed in compact form as follow [38]:

$$AF = \frac{\sin(N\psi/2)}{\sin(\psi/2)} \quad 3.6$$

From equation (3.6) we can reveal the following points about the array factor of a uniform linear array:

1. The principal maximum (major lobe) occurs when , $\psi = 0$; that is,

$$kd \cos \theta_{major} + \xi = 0 \quad \text{Or} \quad \theta_{major} = \cos^{-1}(-\lambda\xi/2\pi d).$$

2. The principal maximum (major lobe) occurs when , $\psi/2 = \pm m\pi$; that is,

$$kd \cos \theta_{major} + \xi = \pm 2m\pi$$

Or

$$\theta_{major} = \cos^{-1}[(\lambda/2\pi d)(-\xi \pm 2m\pi)], \quad m = 0, 1, 2, \dots$$

3. The nulls occur when $\sin(N\psi/2) = 0$; that is, $\frac{N\psi}{2} = \pm n\pi$ for $n = 1, 2, 3, \dots$
and $n \neq N, 2N, \dots$

If the aim is to steer the main beam at $\theta_{major} = 90^\circ$, the progressive phase shift should be equal to zero, provided that $d \neq n\lambda$ for $n = 1, 2, 3, \dots$. If we want the major lobe to appear at $\theta_{major} = 0^\circ$ or $\theta_{major} = 180^\circ$, then (1) for $\theta_{major} = 0^\circ$ the progressive phase shift should be $\xi = -kd$; and (2) for $\theta_{major} = 180^\circ$ $\xi = kd$.

3.3 Planar Array

Linear arrays can only scan the main beam in one polar plane (φ or θ), while planar arrays scan the main beam along both φ and θ . Planar arrays present more gain and lower side-lobes than

linear arrays, but has to use more elements. The design principles for planar arrays are similar to those presented earlier for the linear arrays. Since the elements are placed in two dimensions (see Figure 3.4), the array factor of a planar array can be expressed as the multiplication of the array factors of two linear arrays: one along the x -axis and one along the y -axis [38]:

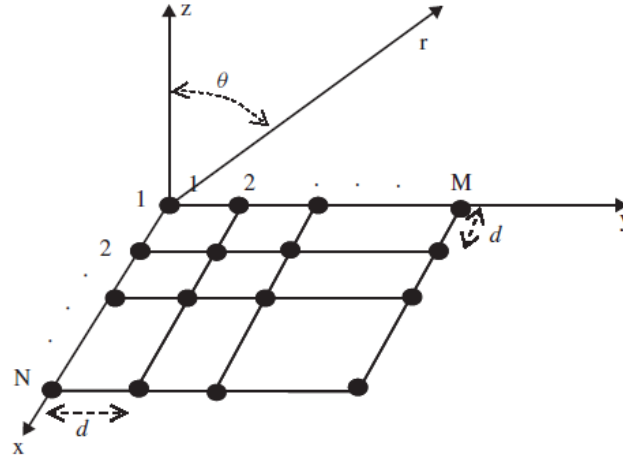


Figure 3.4 Geometry of a rectangular $M \times N$ planar array with interelement distance d [37].

$$AF_{planar} = (AF_x) \cdot (AF_y) \quad 3.7$$

Or

$$AF = \left(\frac{\sin(N\psi_x/2)}{N \sin(\psi_x/2)} \right) \left(\frac{\sin(M\psi_y/2)}{M \sin(\psi_y/2)} \right) \quad 3.8$$

Where

$$\psi_x = kd_x \sin \theta \cos \varphi + \xi_x$$

$$\psi_y = kd_y \sin \theta \cos \varphi + \xi_y$$

By using a progressive phase shift applied to the elements of the array we can scan the main beam in certain angles (phased array), but it is also possible to use different excitation schemes for the individual elements to track multiple sources or targets along θ and φ [37].

3.4 Antenna Beamforming

Beam forming is the capability of the antenna array to focus energy toward a specific direction in space and nulls in the undesired directions. So, beam forming is often referred to as spatial filtering. Just spatial filtering or beam forming was the first approach to carrying out space–time processing of data sampled at antenna arrays [37].

The Bartlett (*conventional*) beam former was the first to stand out during World War II [39]. Later, adaptive beam formers and classical time-delay estimation techniques were applied to improve the ability to resolve closely spaced signal sources [40, 41]. From a statistical point of view, the classical techniques can be seen as spatial extensions of the spectral Wiener (or *matched*) filtering method [42]. However, the conventional beam former has some fundamental limitations connected to the physical size of the array, the available data collection time, and the signal-to-noise ratio (SNR). Some aspects of *analog* and *digital* beam forming are introduced next [37].

3.4.1 Analog Beam Forming

Figure 3.5 illustrates an example of a radiofrequency (RF) beamformer for creating only one beam at the output [43]. In practice, RF beamformers can employ microwave waveguides, microstrip structures, transmission lines, or printed microwave circuits.

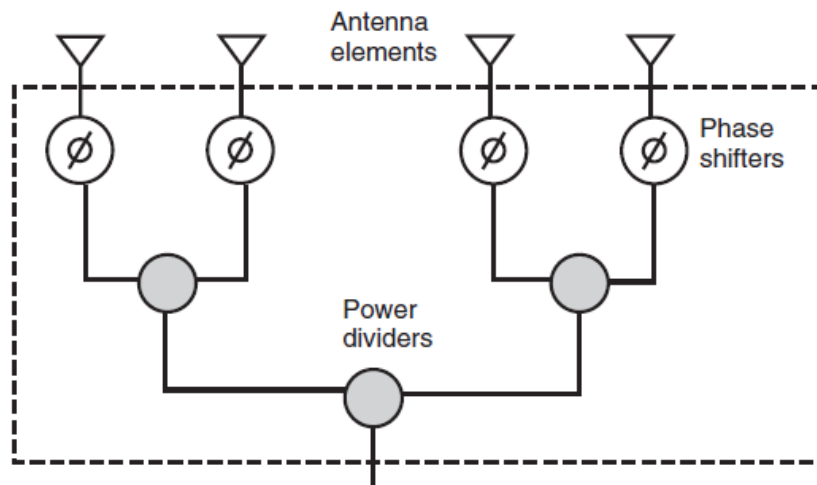


Figure 3.5 Architecture of a simple, on-beam RF beam former [37].

Multiple-beam beam formers are more complex configurations, based mathematically on the beam-forming matrix (the Butler matrix is widely used matrix example [44, 45]). Figure 3.6a

shows a Butler beam-forming matrix for a four-element antenna array. This matrix utilizes two 45° fixed-phase shifters and four 90° phase-lag hybrid junctions. Figure 3.6b illustrates the phasing scheme of the four 90° phase-lag hybrid junctions. Typically, the number of beams is equal to the number of antenna elements in the arrays. By tracing the signal from the four ports to the array elements, one can show that the phase distribution at the antenna aperture corresponds to the individual ports of the four-port Butler matrix. Figure 3.7 depicts the radiation pattern from a four-element antenna array with elements spaced at $\lambda/2$ using a Butler matrix feed structure. Although these four beams are overlapping, they are mutually orthogonal [46].

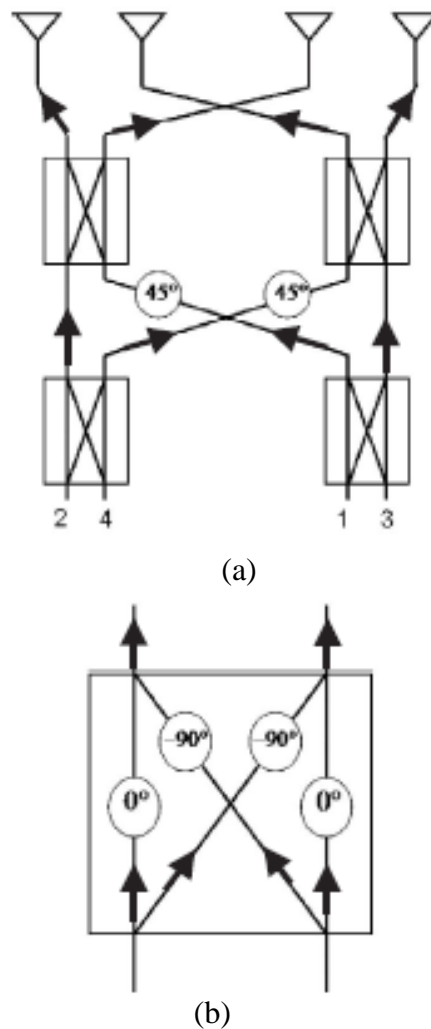


Figure 3.6(a) A Butler beam-forming matrix for a four-element antenna array, and (b) its phasing scheme [37].

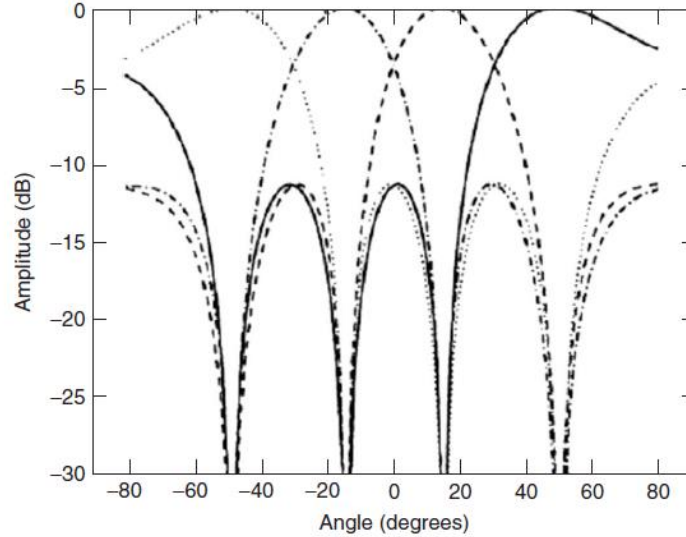


Figure 3.7 Computation of the antenna pattern corresponding to the beam former in Figure 3.6 [46]

3.4.2 Digital Beam Forming

Digital beam forming can be achieved by converting the incident RF signal at each antenna element into two streams of binary complex baseband signals that represent the in-phase component (I) and the 90° phase shifted or quadrature component (Q). These weighted signals, from each element, are sampled and stored, and beams are then formed by summing the appropriate samples [47]. Depending on the choice of weights, one can use this technique to realize a multi-beam antenna array for a switched or an adaptive system. Processing speed and cost have been problems traditionally, but today, inexpensive digital processors, such as field programmable gate arrays (FPGAs), and advanced digital signal processing (DSP) techniques have made the use of smart antennas a reality in wireless communication systems [37]. A simple structure where a processor can be inserted into an antenna array to achieve beam forming is shown in Figure 3.8 [48].

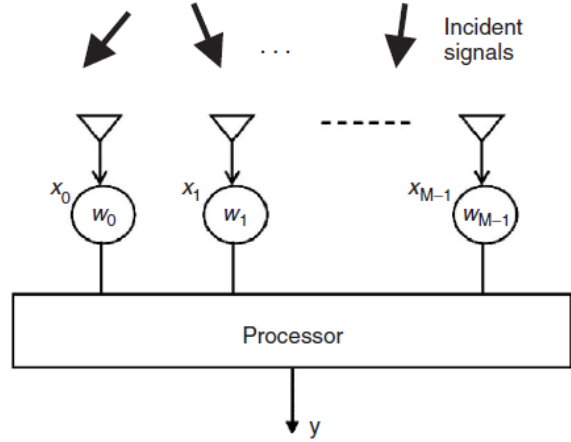


Figure 3.8 Simple digital beam-former architecture [37].

3.5 Means of Phase Shifting

Phased array antenna beam positioning by applying a phase shift to the linear array antenna elements is discussed without specifying how this phase shifting may be achieved. In this subsection we will briefly outline some (certainly not all) methods available for accomplishing a desired phase shift. We first start by identifying the phase of a signal. In all our calculations we have assumed the signals to be time harmonic, i.e. varying according to $e^{j\omega t}$, meaning that a physical realizable signal $s(\omega)$ varies according to the real part of the complex signal $e^{j\omega t}$ [49],

$$S(\omega) \sim \cos(\omega t) \tag{3.9}$$

Where $\omega = 2\pi f$, f being the frequency of the signal. The argument of the cosine is known as the *phase*, ψ . The time t may be expressed as the ratio of distance, l , to velocity of the signal, c , where $c = \frac{1}{\sqrt{\epsilon\mu}}$, so that we find for ψ [49]

$$\psi = 2\pi f l \sqrt{\epsilon\mu} \tag{3.10}$$

Where ϵ is the permittivity of the medium which the signal is travelling through and μ is the permeability of this medium [49]. This equation reveals all phase-shifting possibilities at a glance.

The possibilities are:

1. Phase shifting by changing frequency.
2. Phase shifting by changing length.

3. Phase shifting by changing permittivity (dielectric constant).
4. Phase shifting by changing permeability.

3.5.1 Phase Shifting by Changing Frequency

Phase shifting by changing frequency or *frequency scanning* is accomplished by series feeding the array antenna elements, having the elements equidistantly positioned along the line and changing the frequency [49], see Figure 3.9.

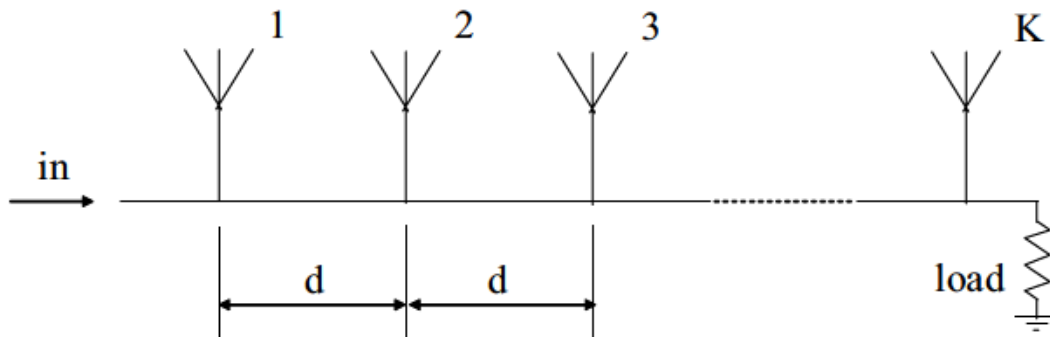


Figure 3.9 Series-fed linear array antenna consisting of K identical elements, equidistantly displaced d with respect to one another [49].

We have seen that changing the frequency makes the phase change. Another way of looking at this phase change is taking the *electrical length* into account. Using $c = \frac{1}{\sqrt{\epsilon\mu}}$, $f = \frac{c}{\lambda}$ and $k = \frac{2\pi}{\lambda}$, substituted into equation (3.10), results in

$$\psi = kl \tag{3.11}$$

Which is known as the *electrical length*.

From the last equation, we note that by changing the frequency (parameter in k), we create a changing linear phase taper over the array antenna elements, since the input signal in Figure 3.9 has to travel over a physical length l_i and electrical length kl_i to reach the i^{th} element of the K -elements linear array antenna. If the physical lengths of the feeding lines are chosen such that at the center frequency, the phased array antenna beam is directed to broad sight. So that, we can change the frequency to values lower than and greater than the center frequency to get the beam directed to, respectively, angles smaller than and angles greater than broad sight [49].

3.5.2 Phase Shifting by Changing Length

Another way of accomplishing a desired phase shift is by changing physical lengths, as equation (3.10) reveals. This type of phase shifting may be applied to series-fed arrays as in Figure 3.10,a,b, or to corporate-fed arrays as Figure 3.10,c [50].

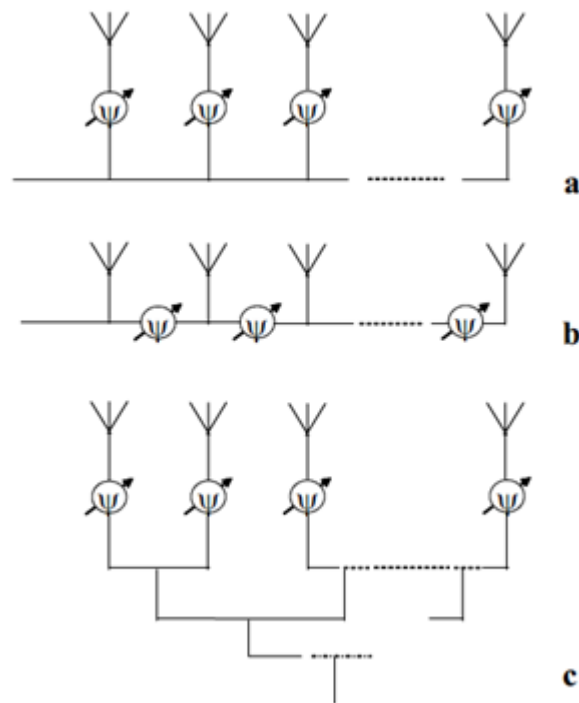


Figure 3.10 Phase shifters in a linear phased array antenna feed network. a, b. Series-fed linear phased array antenna. c. Corporate-fed linear phased array antenna [49].

The *line stretcher* [51] is an example of an early type phase shifter. The line stretcher is a (coaxial) transmission line section, bent in the form of a ‘U’. The bottom part of this ‘U’ is connected to the two ‘arms’ that form part of the stationary feeding network. The bottom part of the ‘U’ acts as a telescoping section that may be stretched by electromechanical means, thus lengthening and shortening the transmission line section, without changing the position of the ‘arms’ of the ‘U’. Nowadays, different lengths of transmission line are selected digitally. A schematic view of a cascaded, four-bit, digitally switched phase shifter is shown in Figure 3.11. The switches in every section are used to either switch a standard length of transmission line into the network or a piece of transmission line that adds to this standard length a piece of predetermined length [50, 51]. These lengths are chosen such that when the cascade of standard length is taken as reference,

having a phase $\psi = 0^\circ$, 16 phases (4 bits), ranging from $\psi = 0^\circ$ to $\psi = 337.5^\circ$, in steps of 22.5° . The least significant bit (LSB) may be selected [49].

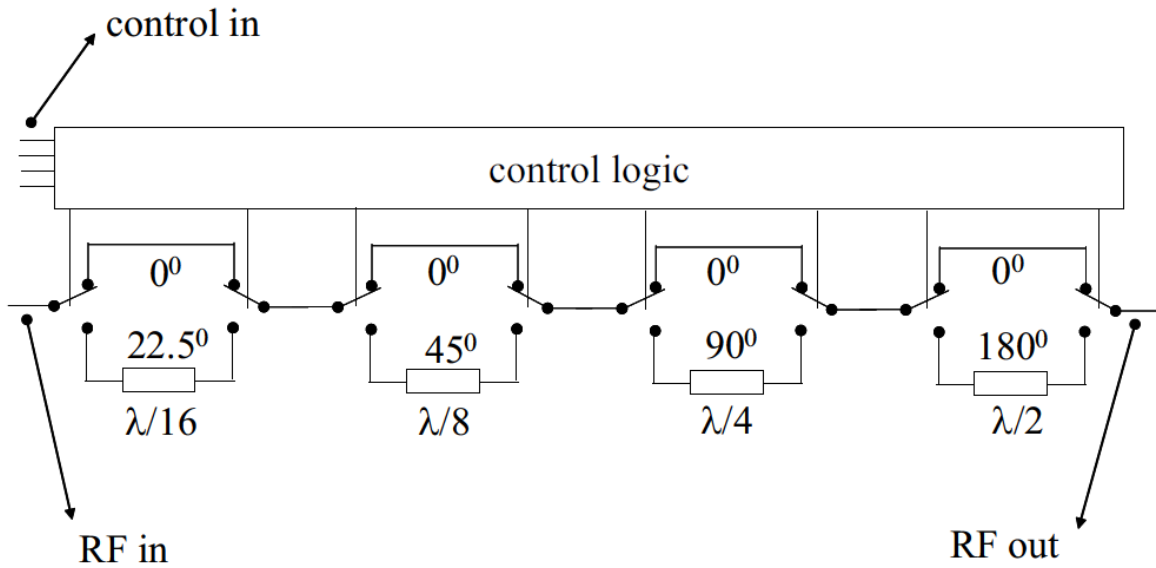


Figure 3.11 Cascaded, four-bit, digitally switched phase shifter [49].

3.5.3 Phase Shifting by Changing Permittivity

As equation (3.10) shows that a phase shift may be achieved by changing the permittivity, ϵ , or dielectric constant of the material a signal is propagating through. One way is to use a gaseous discharge or plasma, where the dielectric constant – and thus the phase shift - is changed by changing the current through the device [51]. Another way is provided by making use of so-called *ferroelectric* materials. Ferroelectric materials are materials having permittivity function of the applied electric field over the material [49].

3.5.4 Phase Shifting by Changing Permeability

Equation (3.10) shows that a change in permeability, μ , works equally well in changing the phase. *Ferromagnetic* materials, or *ferrites* are materials which its permeability changes as function of the change in an applied magnetic field in which the material is positioned. Ferrite-based phase shifters have been in use for a long time, especially in combination with waveguide transmission line technology [49].

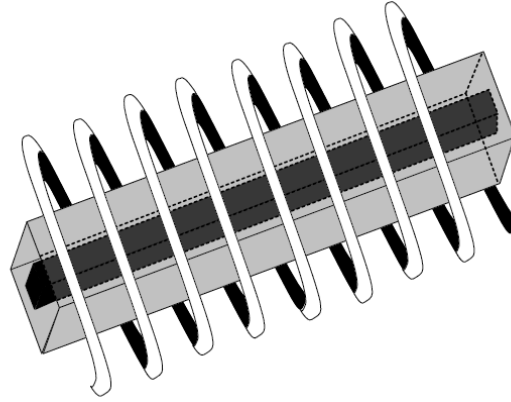


Figure 3.12 Basic Reggia–Spencer phase shifter configuration [49].

The *Reggia–Spencer phase shifter*, in its basic form, consists of a rod of ferromagnetic material, centrally positioned inside a waveguide, where a solenoid is wound around the waveguide, see Figure 3.12 [50, 51]. By changing the current through the solenoid, the magnetic field is changed and thereby the permeability of the ferromagnetic rod and thus the phase of a wave going through the waveguide is changed. The phase can be changed continuously, making the Reggia-Spencer phase shifter an *analog* phase shifter. A section (bit) of a *digital* ferromagnetic phase shifter is shown in Figure 3.13 [50, 51].

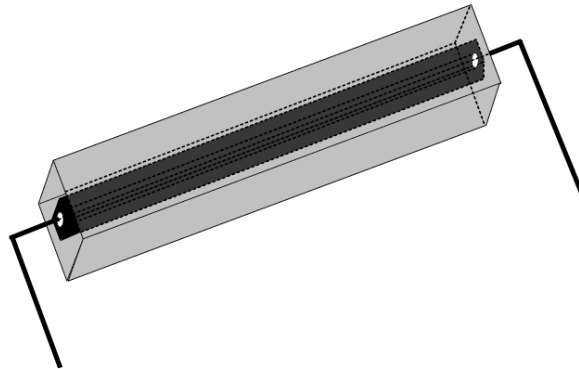


Figure 3.13 Single section (bit) of a latched ferrite phase shifter [49].

The function of the solenoid is taken over by a current wire through the ferromagnetic rod. By cascading different lengths of ferromagnetic rods, different (discrete) phase shifts may be realized [49].

3.6 Phased Array Architecture

3.6.1 Phased Arrays based on feed network design

Phased arrays are usually composed of a feed network and a number of phase shifters and the radiators elements. Feed networks are used to distribute the output signal of the transmitter to the radiation elements and phase shifters control the phase of the signals at each radiating element to form a beam at the desired direction. There are almost as many ways to feed arrays as there are arrays in existence. In general, array feed networks can be classified into three basic categories: constrained feed, space feed and semi constrained feed which is a hybrid of the constrained and the space feeds [52]. In a space feed network, the array is usually illuminated by a separated feed horns located at an appropriate distance from the array [53]. Due to the free space existing between the feed and radiating elements, this type of feed network is not a good candidate for planar arrays. The constrained feed, which is usually the simplest method of feeding an array, generally consists of a network which takes the power from a source and distributes it to the antenna elements with a feed line and passive devices. The constrained feed itself can be categorized into two basic types: parallel feeds and series feeds [54]. The architectures based on these two types of feed network are the most common approach to design phased arrays [2].

a. Parallel-fed Arrays

In parallel feed networks, which are often called corporate feeds, the input signal is divided in a corporate tree network to all the antenna elements as shown in Figure 3.14. These networks typically employ only power dividers [55]. Therefore their performance critically depends on the architecture of the power splitter/combiner used [2].

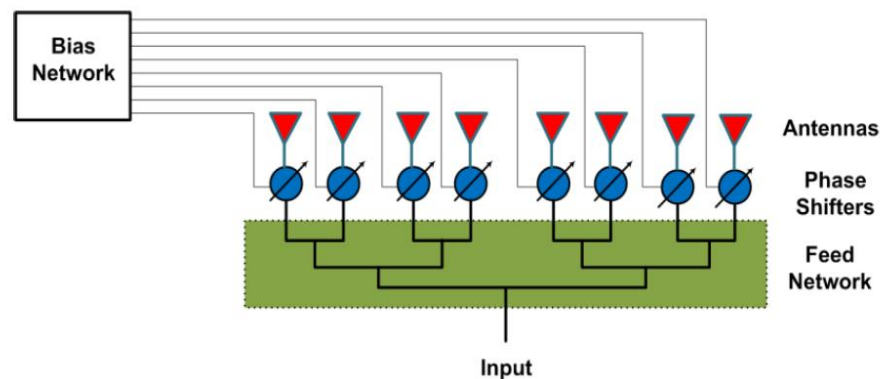


Figure 3.14 General diagram of parallel fed phased array [2].

b. Series-fed Arrays

In a series-fed array the input signal, fed from one end of the feeding network, is coupled serially to the antenna elements as shown in Figure 3.15. The compact feed network of series-fed antenna arrays is one of the main advantages that make them more attractive than their parallel-fed counterparts.

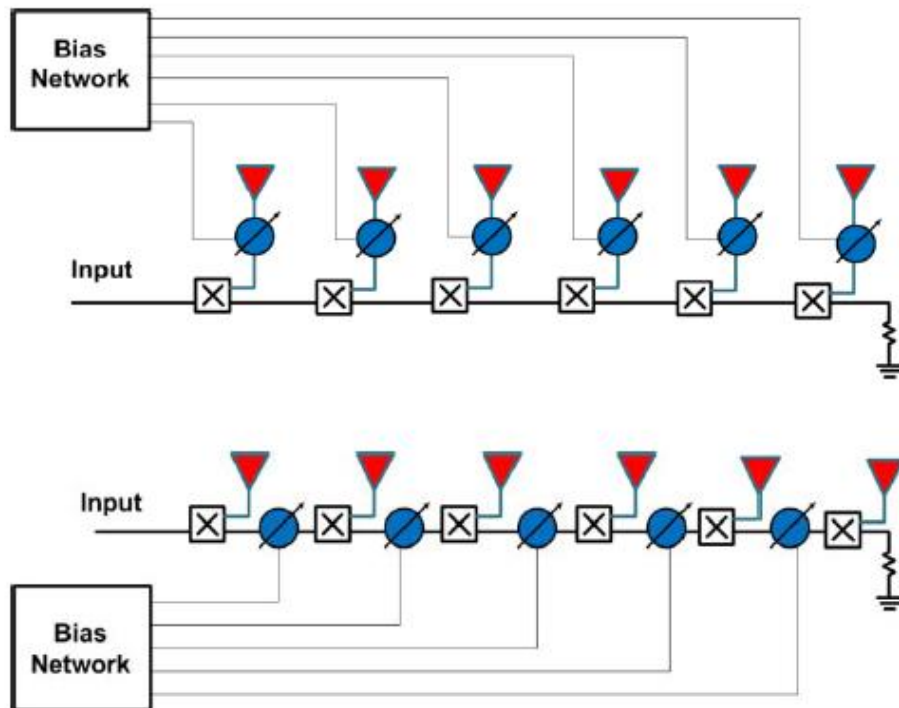


Figure 3.15 General diagram of series fed phased array [2]

Beside compactness, the small size of series-fed arrays gives less insertion and radiation losses which caused by the feed network [56]. The cumulative nature of the phase shift in series arrays also relaxes the design constraints on the phase tuning range of the phase shifters. In an N -element series-fed array, the required amount of phased shift is smaller than parallel fed arrays by a factor of $(N-1)$. However, the cumulative nature of phase shift through the feed network results in an increased beam squint versus frequency [34], which is one of the main limitations in series-fed designs. The loss through the phase shifters is another cumulative value in series fed arrays which can be an issue in the design of arrays with a large number of array elements [2].

3.6.2 Phased array based on phase shift stage

Phase shifters can be placed at any stage of phased array system. Based on the stage in which phase shifting is placed, phased arrays can be classified into four distinct types: Radio Frequency (RF)-phase shifting, Local Oscillator (LO)-phase shifting, Intermediate frequency (IF)-phase shifting and digital phased arrays. In the following points, each of these types of phase arrays will be discussed briefly [2].

3.6.2.1 Means of Converters

In electronics, a local oscillator (LO) is an electronic oscillator used with a mixer to change the frequency of a signal. This frequency conversion process produces the sum and difference frequencies from the frequency of the input signal. Processing a signal at a fixed frequency gives a radio receiver improved performance. In many receivers, the function of local oscillator and mixer is combined in one stage called “converter”, this reduces the space, cost and power consumption by combining both functions into one active device.

3.6.2.2 RF phase shifting

Figure 3.16 presents the general architecture of phased arrays using RF phase shifting. In this architecture, the signals at the antenna elements are phase-shifted and combined in the RF domain. The combined signal is then down converted to baseband using heterodyne or homodyne mixing [2].

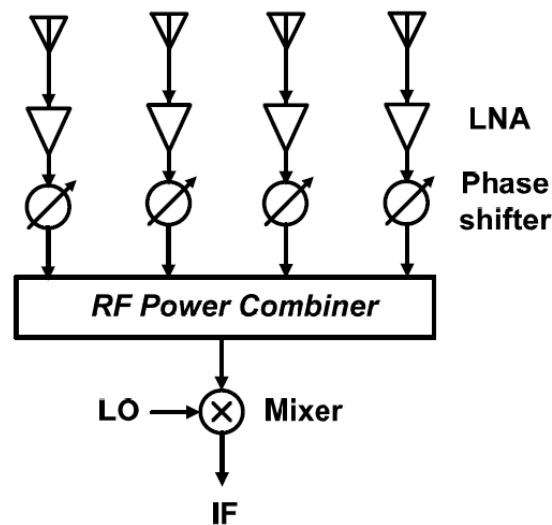


Figure 3.16 General diagram of RF phase shifting phased array [2].

Designing phased arrays using RF phase-shifting has been traditionally more common compared to the other architectures. Since this technique requires only a single mixer and there is no need of LO signal distribution, it usually results in the most compact architecture among other phase array designs [57]. The main challenge of using phase shifting at RF stage in the design of phased arrays is implementing high performance phase-shifters capable of operating at RF frequencies. Furthermore, phase shifter used in receive phase arrays are in the RF signal path and therefore, their noise performance can be critical for the sensitivity of receivers [2].

3.6.2.3 LO phase shifting

Figure 3.17 shows the general architecture of phased arrays based on LO phase shifting. The phase of RF signal at each channel is basically the sum of phases of IF and LO signals. Therefore, tuning the phase of LO signals will change the phase of RF signals [2].

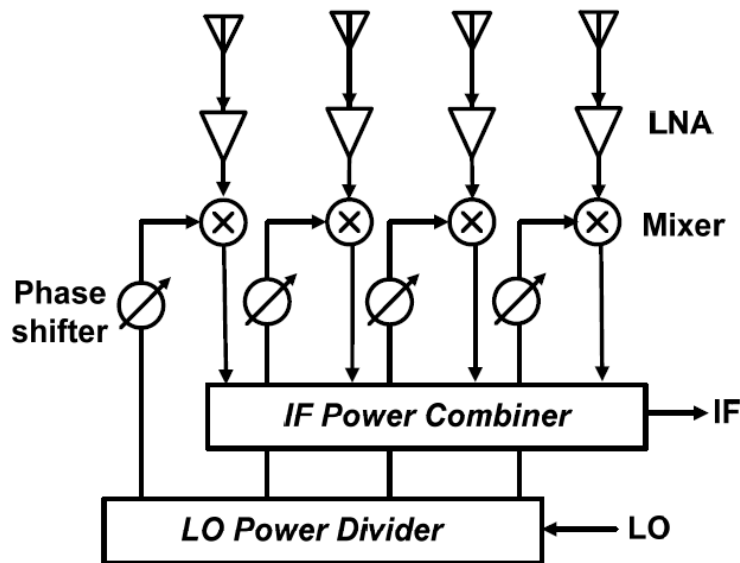


Figure 3.17 General diagram of LO phase shifting phased array [2].

The advantage of this approach compared to other architectures is that the phase-shifters are not placed on the signal path [58, 59]. As a result, the loss, nonlinearity and the noise performance of the phase-shifters would not have a direct impact on the overall system performance. Furthermore, performance of the required phase shifter on LO signal path, such as bandwidth, linearity and noise figure will not be as stringent as the phase shifters on the signal path [60]. However, this method compared to RF phase shifting requires a large number of mixers, therefore; in general, the overall

complexity and power consumption will be higher than phased arrays based on RF stage phase shifting [2].

3.6.2.4 IF phase shifting

The general architecture of phased arrays based on IF phase shifting is shown in Figure 3.18. As we mentioned before, the phase of RF signal at each channel is the sum of phases of IF and LO signals. Therefore, tuning the phase of RF signals can be achieved by tuning through tuning the phase of IF signal [61, 62]. The main advantage of this approach over RF and LO phase shifting is that the phase-shifting is performed at much lower frequencies, therefore, designing phase shifters with much better performance can be possible at IF path. As a result, the loss, nonlinearity and the noise performance of the phase-shifters can be much better when IF phase shifting is used. However, in this architecture similar to LO phase shifting phased arrays large number of mixers are required that can add to the overall system complexity and its power consumption. Furthermore, since the interfere cancellation occurs only after the IF stage, all the mixers are required to have a high level of linearity capable of handling strong interference emanating from undesired directions [2].

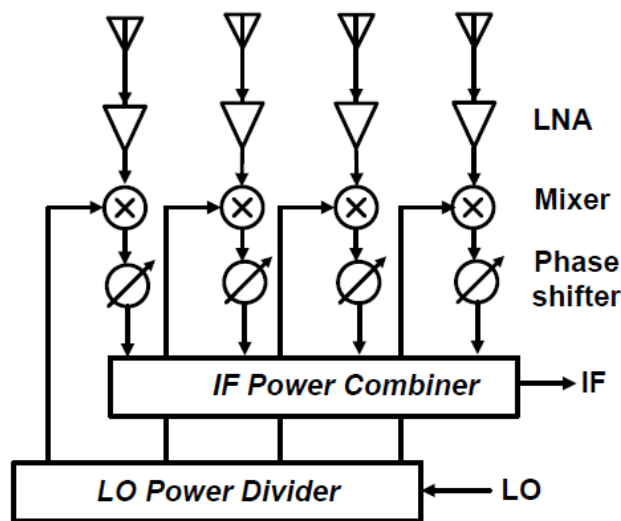


Figure 3.18 General diagram of IF phase shifting phased array [2]

3.6.3 Primary and secondary array

As can be seen in Figure 3.19, the array elements are divided into the groups of in-phase elements, or sub-arrays, referred to as a primary array. Each of the primary arrays assuming to be identical uses a single phase shifter.

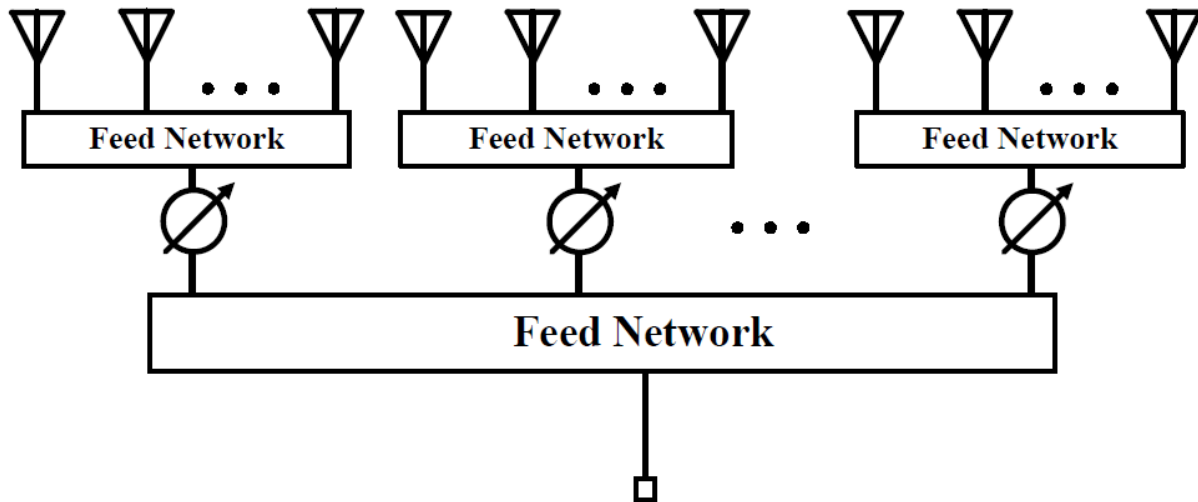


Figure 3.19 Grouping antennas into a sub array each using one phase shifter can reduce the number of required phase shifters [2]

Furthermore, each of these primary arrays can be viewed as the elements of a second phased array called the secondary array. The array factor for the overall structure will be equal to the product of these two array factors [2].

3.7 Conclusion

In this chapter, the concept of phased array antenna is presented. In section 4, the concept of beamforming and its types are presented. In section 5, the means of phase shifting techniques are presented. Section 6 presented common architectures for phased array showing their advantages and disadvantages. In chapter 4, the design of a phased array system for beam steering will be introduced and the results will be discussed.

4. Design and Implementation

4.1 Introduction

In this chapter, a new method to design phased arrays based on hybrid couplers technique is presented. In this method, power dividing and phase shifting tasks are performed using the same circuitry. Unlike the conventional phased arrays which shown in Figure 4.1 where there is a need for a separate phase shifter per each antenna element, this technique eliminates this requirement hence reducing phased arrays complexity (Figure 4.2). In the design of the phased array, hybrid coupler is utilized with heterodyne mixing to achieve uniform power distribution at the Intermediate Frequency (IF) paths and to perform phase shifting at the IF-stage.

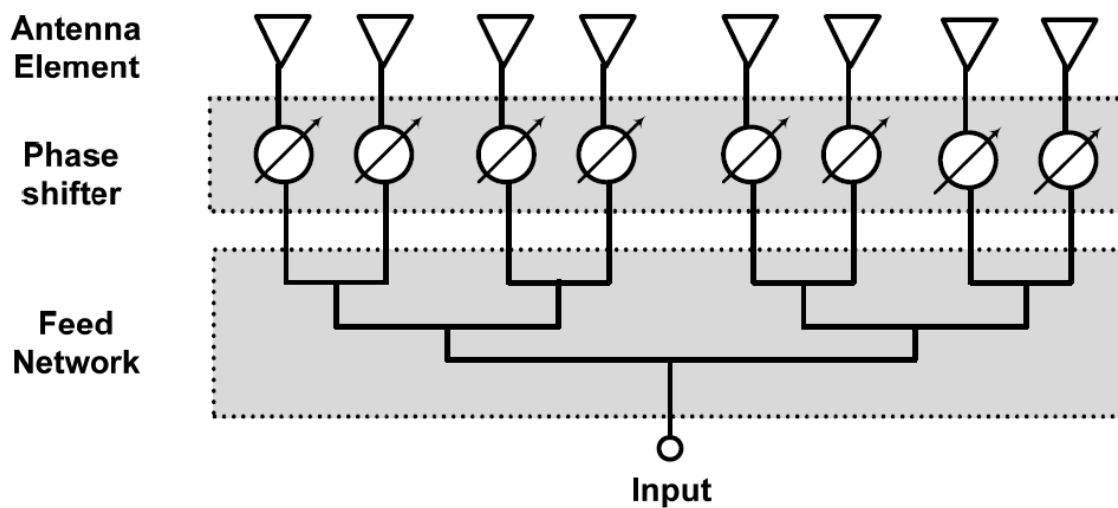


Figure 4.1 The conventional design of phased arrays requires one phase shifter for each antenna element [2].

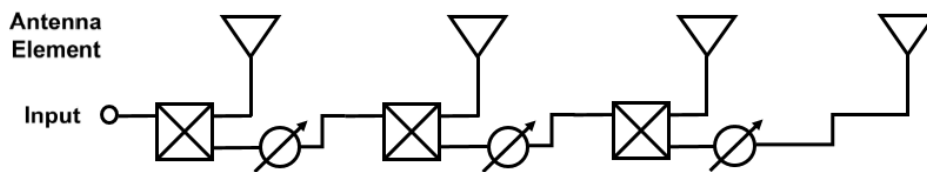


Figure 4.2 In hybrid couplers phased array, phase shifters and power dividing network are combined in a single entity

In order to steer the beam, the phase shift between the Radio Frequency (RF) signals can be tuned by utilizing varactors in the IF or Local Oscillator (LO) networks. Phase shifting at the IF stage (Figure 3.18) is preferred due to the better performance of varactors at lower frequencies. The tunable IF modules are realized based on hybrid couplers circuit topology shown previously.

The signal at an IF port can be presented by equation 4.1 [2]

$$S_{IF(n)} = A_{IF} \cos(w_{IF}t + n\theta_0 + n\Delta\theta) \quad 4.1$$

where, A_{IF} is the amplitude of the IF signal, w_{IF} is the angular frequency of the IF signal, θ_0 is the progressive phase shift in IF circuit, $\Delta\theta$ is the external phase shift due to the phase shifters. Furthermore, the signal at the corresponding LO port is given by

$$S_{LO(n)} = A_{LO} \cos(w_{LO}t + n\phi_0) \quad 4.2$$

where, ϕ_0 is the initial phase shift in LO circuit. Therefore, the signal fed to the corresponding antenna element can be obtained using equation 4.3 assuming the mixer gain to be A_{mixer} .

$$S_{RF(n)} = A_{mixer} A_{LO} \cos((w_{IF} + w_{LO})t + n\phi_0 + n\theta_0 + n\Delta\theta) \quad 4.3$$

Therefore, the frequency of RF transmit signal is given by

$$W_{RF} = W_{IF} + W_{LO} \quad 4.4$$

Furthermore, the initial phase progression across the IF ports is canceled out by the phase progression across the LO ports allowing scanning around the broadside. Therefore, the relationship given by equation 4.5 should be met to set the initial beam corresponding to the mid tuning range at broadside.

$$\phi_0 = -\theta_0 \quad 4.5$$

4.2 IF Circuit Design

In [2], the array feeding network is designed to distribute the power and to achieve the phase shift at the same time using extended resonance method. In this thesis, the IF-network is designed at 1.7 GHz, and it is composed of three tunable phase shifters, four IF ports, and three hybrid couplers for power dividing. The IF power dividing circuit is shown in Figure 4.3.

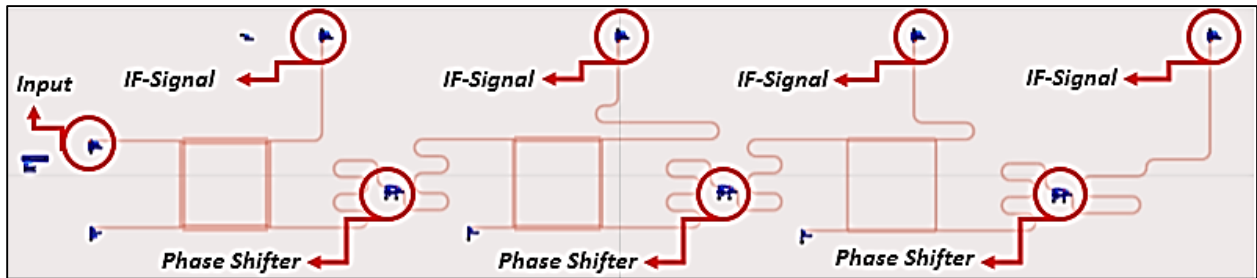


Figure 4.3 The IF distribution network at 1.7 GHz

The first coupler divides the input signal into two ports with ratio of 1:4; one for IF-signal port and the other for entering as an input for the second coupler. The second coupler divides the signal into two ports with ratio of 1:3; one for IF-signal port and the other for entering as an input for the third coupler, which divides the signal into another two IF-signal ports with ratio of 1:2. Phase shifters are located between every two adjacent couplers in order to change the phase. Series feeding allow us to have fixed phase shift between every adjacent ports. Signal will arrive to port four through three phase shifters with 3ϕ , and to port three through two phase shifter with 2ϕ , and to port two through one phase shifter with ϕ . Figure 4.4 illustrate the delays between the elements of array.

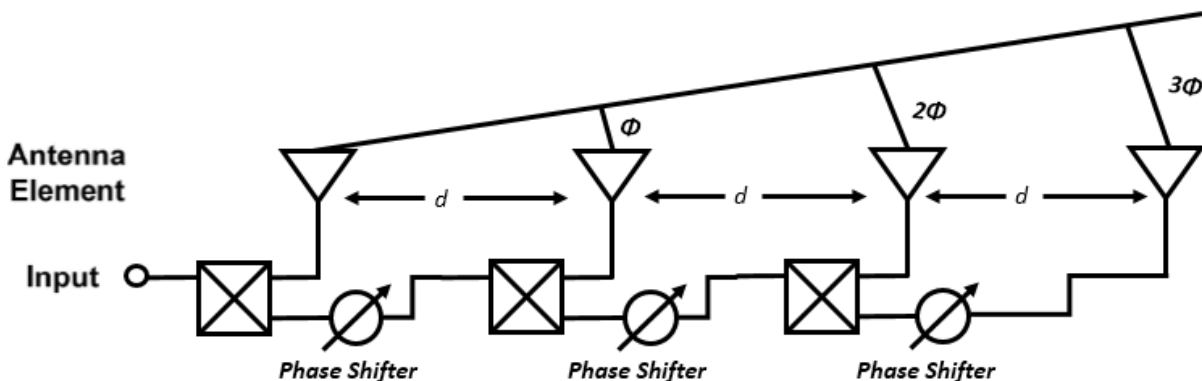


Figure 4.4 Phases between the antennas element

4.3 Phase Shifters Design

Phase shifters are the key blocks in this project. Here, the phase shifter consists of a series inductor connected to two capacitors in shunt. The inductance value of the inductor is 5.4 nH, this value is chosen after some iterations to achieve the optimized case of having larger phase shift with lower insertion loss. Figure 4.5, illustrates the structure of phase shifter. As we can see, there are two transmission line in the input and output port for having a linear values of phase shifts across the zero degree. In order to change the phase shift between the input and output, the values of capacitors are varied. In our case, we tune the applied voltage on the varactors.

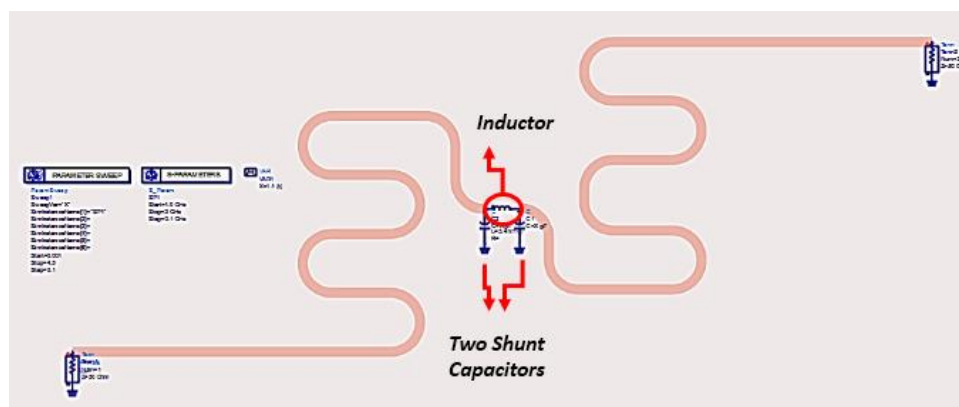


Figure 4.5 IF Phase shifter

The insertion loss of the phase shifter with sweeping the capacitance value is shown in Figure 4.6. We note from the figure that if the capacitance increases above 4.5 pf the insertion loss becomes larger than acceptable, so that we have to keep the value of the capacitance below 4.5 pf.

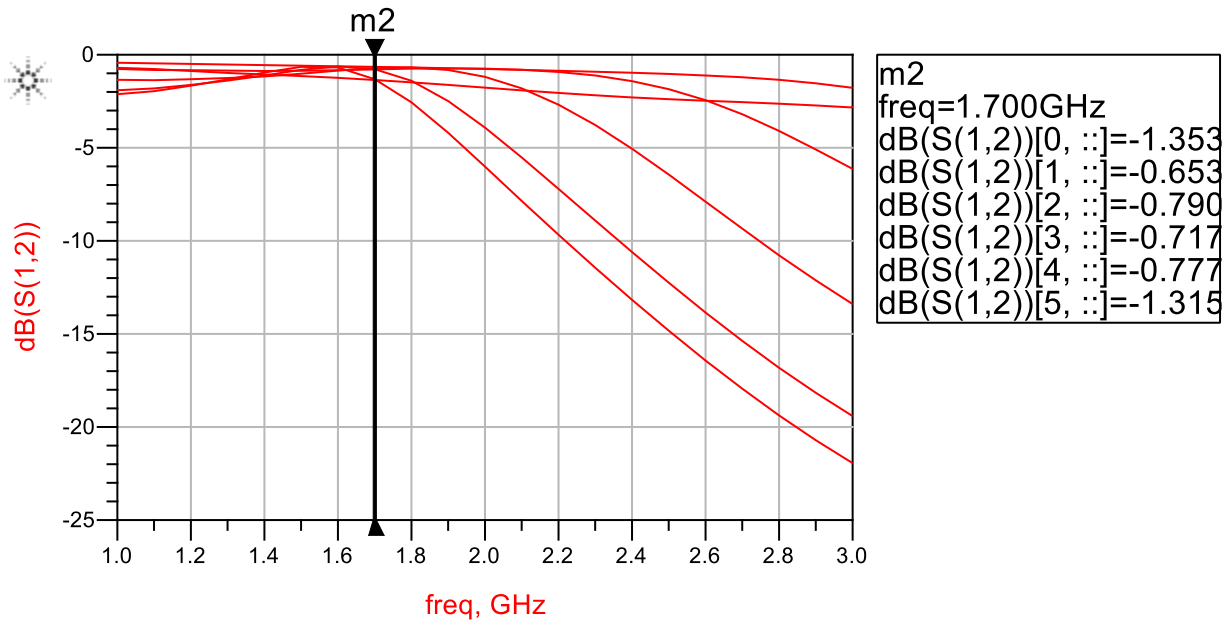


Figure 4.6 Phase shifter insertion loss

Phase shifts result from the designed phase shifter is shown in Figure 4.7. The maximum phase shift is about 62 degree and the minimum is -98 degree.

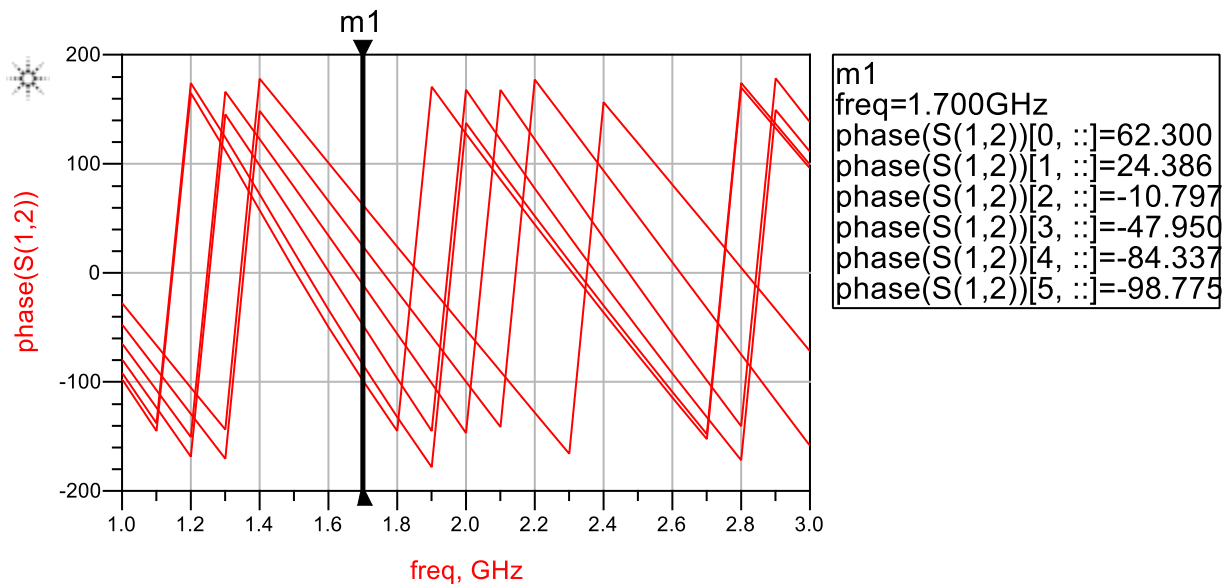


Figure 4.7 Phase shifts with varying the capacitance

In addition to IF signal distribution, the power dividing circuit provide the required phase shift to steer the beam. The phase shift can be controlled by tuning the reverse voltage applied on varactors. The capacitance of the BB833 varactors can be tuned from 0.6 pF to 8.5 pF as the bias voltages

change from 1 volts to 28 volts as shown in Figure 4.8. See appendix A for BB833 varactors datasheet.

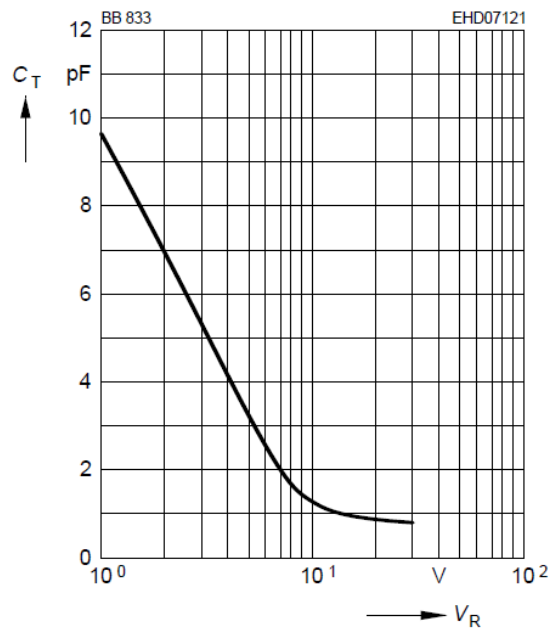


Figure 4.8 BB833 varactor Capacitance versus applied voltage

Advanced Design System 2014.01 (ADS) is used in order to do the simulation of the IF-circuit. 0.47mm height, 0.01 tangent loss and 4.1 dielectric constant of FR-4 substrate material is used. The result of scattering parameters simulation is illustrated in Figure 4.9 .Ideally, the value of the transmission coefficient distributed to each IF-port -6.02 dB (a quarter of input signal strength), and but simulation results show a value around -8dB. As we can see there is 2 dB due to the losses in the substrate material and in phase shifters. Figure 4.10 presents the phase shifts between the adjacent ports when the angle of steering is zero degree. The initial phase across the IF ports which have to be cancelled is 14.5 degree as shown in Figure 4.11.

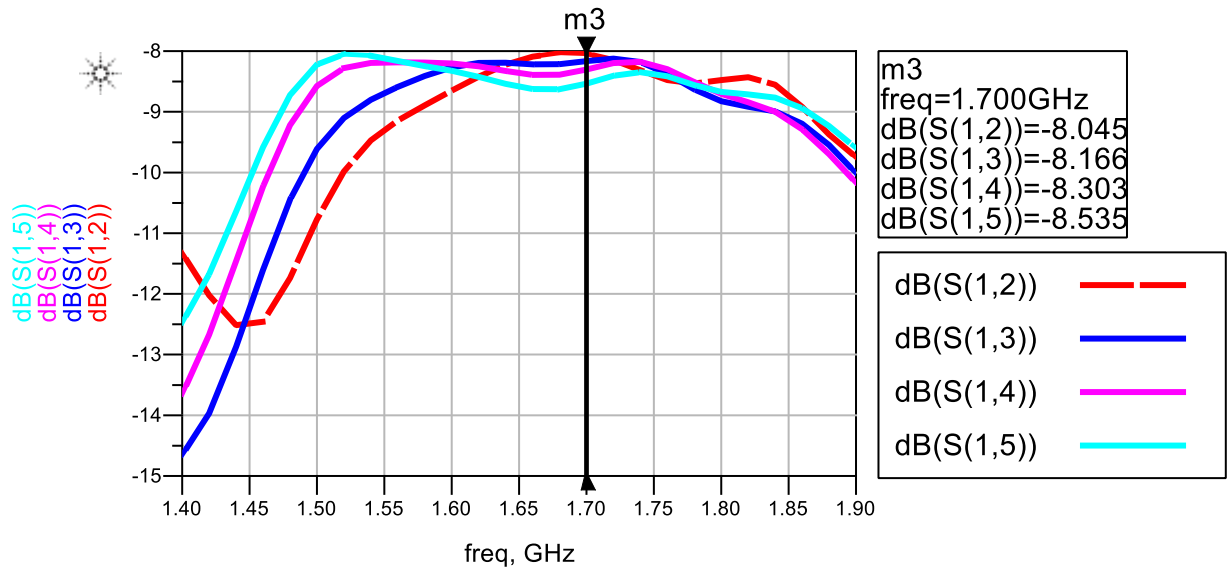


Figure 4.9 Scattering parameters simulation results

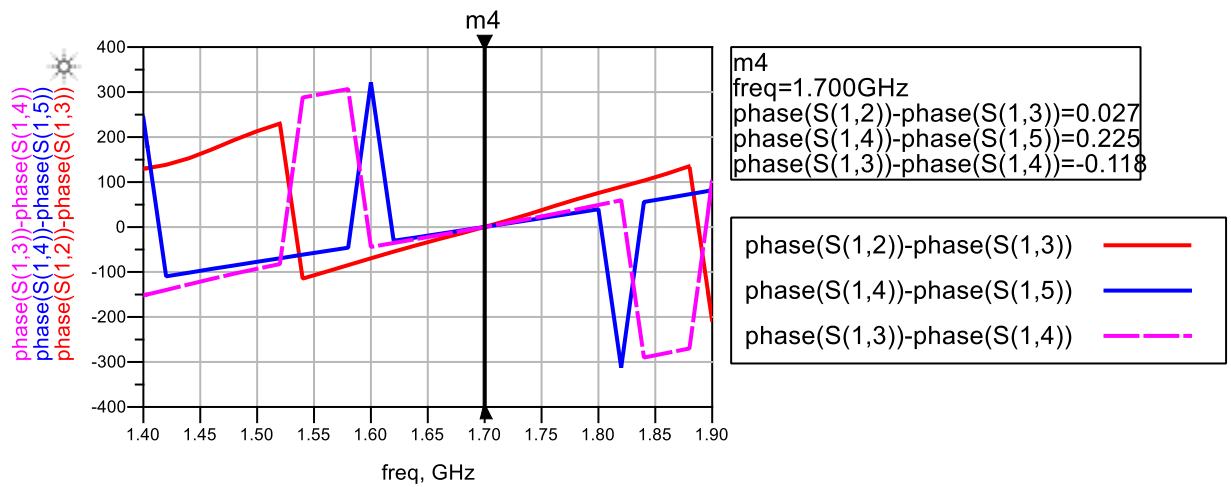


Figure 4.10 Phase shift between adjacent ports

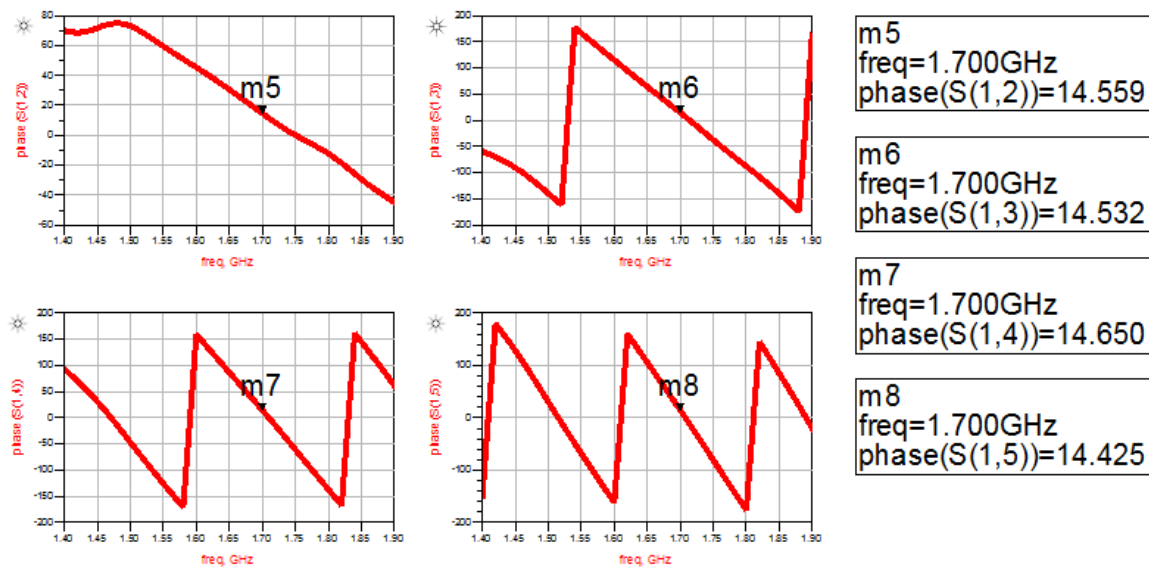


Figure 4.11 The initial phase progression across the IF ports

4.4 Antenna design

Microstrip patch antennas are used as radiating elements in the presented phased array. The patch antenna at the center frequency of 12.3 GHz was designed. In order to test the IF-circuit, patch antenna at center frequency of 1.7 GHz was designed. Based on this procedure, dimensions of the antenna are extract by the equations 2.21-2.24.

4.4.1 Design L-band antenna

The L-band patch antenna with its dimensions is shown in Figure 4.12. The simulated 2D radiation pattern of the antenna is shown in Figure 4.13. The Gain of the antenna is about 2.02 dB and the Directivity is 5.75 dB. Beamforming will be done using this antenna in an array in order to test our distribution circuit.

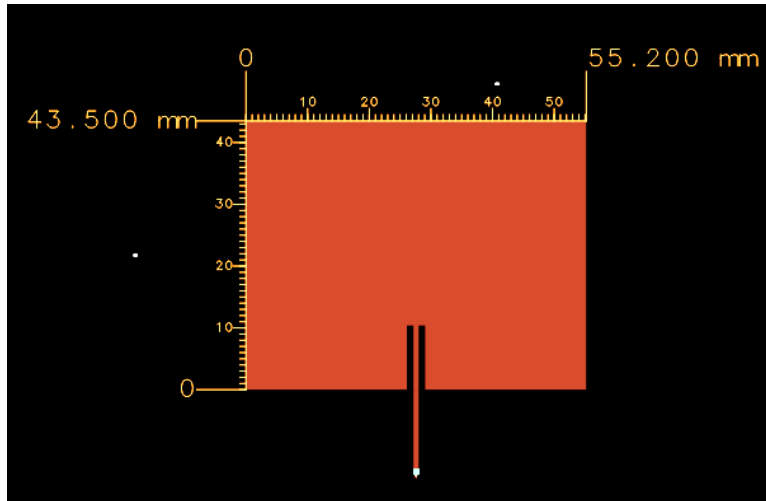


Figure 4.12 L-Band Antenna Dimensions

The antenna is designed to be matched to 50 ohm. The simulated return loss of antenna is shown in Figure 4.14. The -10 dB bandwidth is very narrow but it does not matter because it is just for testing the steering.

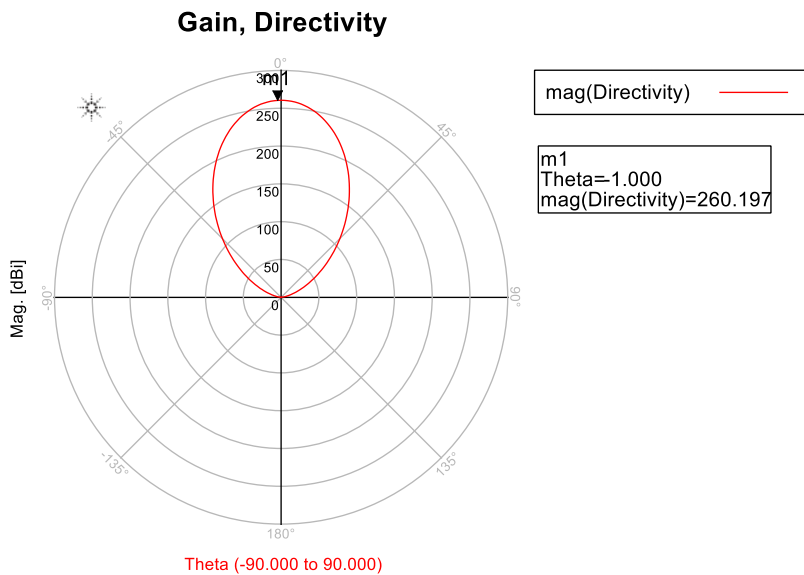


Figure 4.13 2D Radiation Pattern of L-Band Antenna

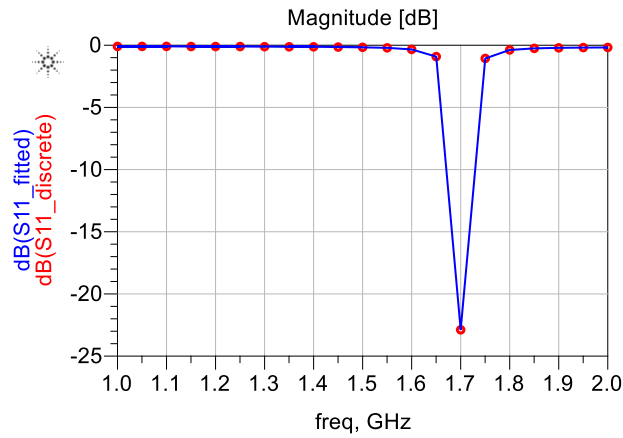


Figure 4.14 Return Loss of L-Band Antenna

The circuit in Figure 4.3 will be used to distribute the IF-signal with the same amplitude and with adaptive phase shift to 4-element L-band antennas array.

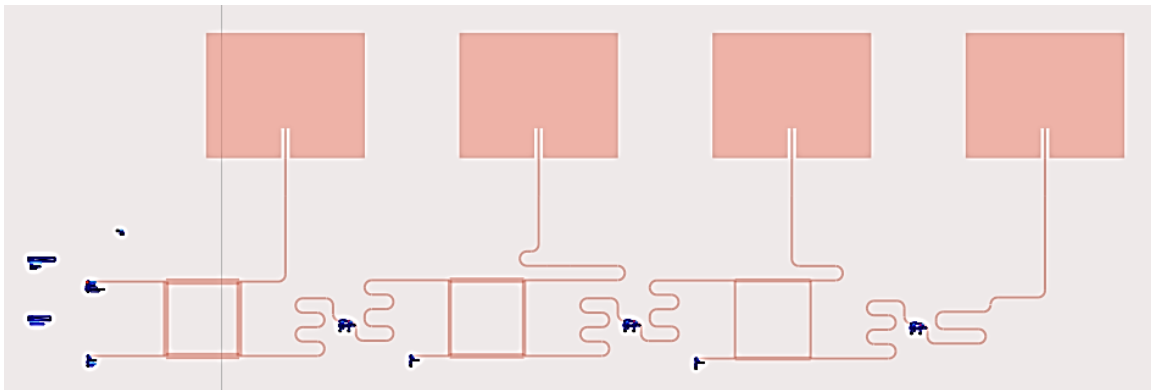


Figure 4.15 Beamforming array at L-band domain

Figure 4.15 illustrates the phased array antenna with steering circuit. The maximum radiation pattern value will be at theta equal to zero when the value of varactors capacitance equal to 1.5 pF that is when the applied reverse voltage equal to 10 VDC as we can see from Figure 4.8.

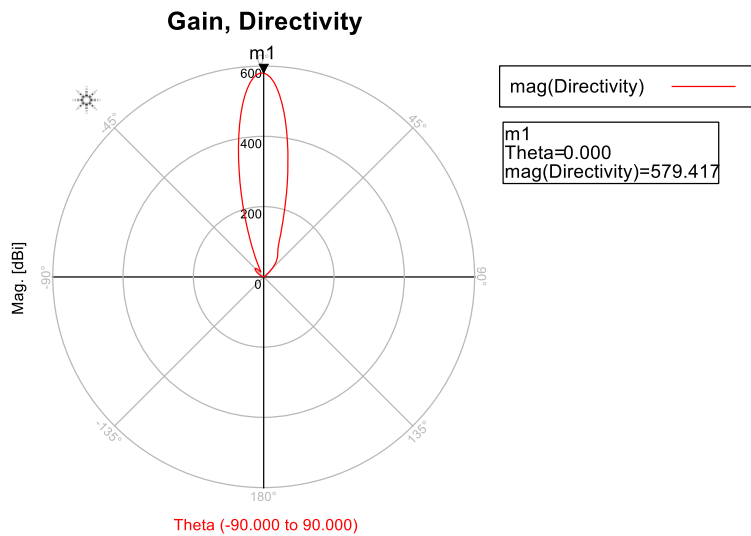


Figure 4.16 Radiation pattern when $C=1.5 \text{ pF}$

The gain of the overall system is about 7.98 dB and the directivity about 11.2 dB. To do steering, we vary the reverse applied voltage in the varactors in order to have a capacitance about 0.001 pF and notice the variation of the radiation pattern angle.

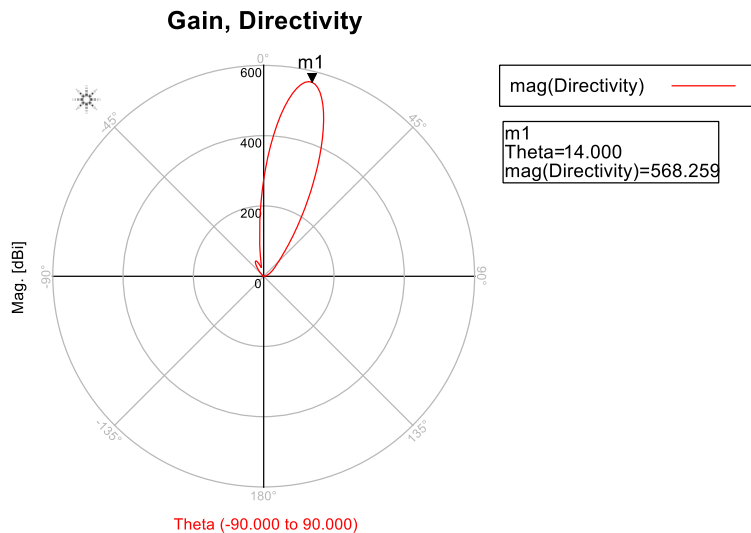


Figure 4.17 Radiation pattern when $C=0.001 \text{ pF}$

Figure 4.17 illustrates the radiation pattern of the maximum steering angle which is about 14 degree. So as we can see, when the capacitance fall from 1.5 pF to 0.001 pF the scan angle increased from 0 to 14 degree. Now, we want to have the maximum capacitance value which does

not effect on the shape of radiation pattern. By varying the capacitance to 4.5 pF the radiation pattern will have its maximum value at -36 degree as we can see from Figure 4.18.

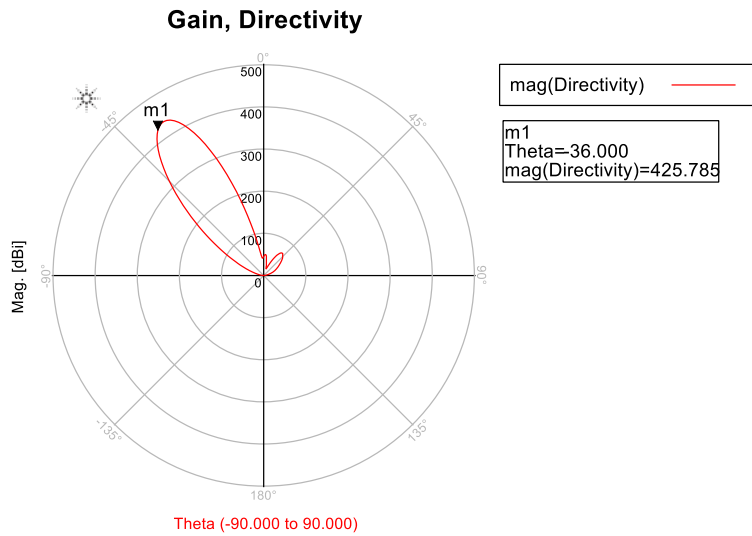


Figure 4.18 Radiation pattern when $C=4.5$ pF

The use of varactors in this system allows us to have a continuous steering angle from -36 to 14 degree. As an example, we can select varactors capacitance of 3 pF to have an angle of -14 degree.

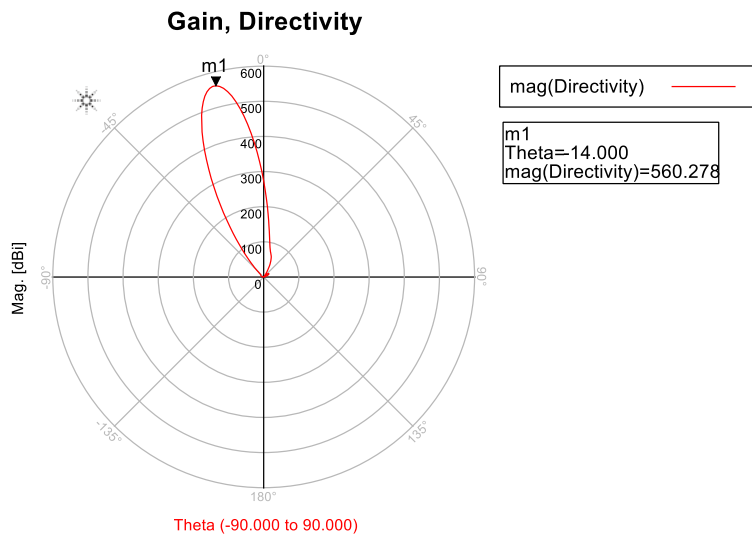


Figure 4.19 Radiation pattern when $C=3$ pF

The radiation pattern of the phased array when the capacitance is 3 pF is illustrated in Figure 4.19. The angle of 10 degree is achieved by adjusting the varactors capacitance to 0.5 pF as we can see from Figure 4.20.

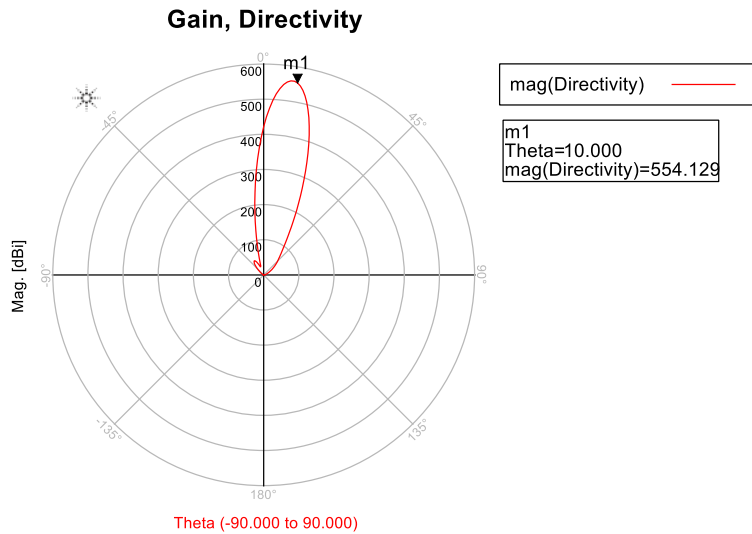


Figure 4.20 Radiation pattern when $C=0.5 \text{ pF}$

4.4.2 Beam Steering with enhanced gain phased array antenna

We can improve the overall system gain by increasing the number of array elements or by increase the gain of the single element itself [4]. Figure 4.21 presents an array of two elements of the L-band antenna. The gain of the two elements array is 4.8 dB. The two elements array will be used in the overall array as a subarray as depicted in Figure 4.22. The gain and directivity of the two array antenna is about twice in magnitude of single element antenna, in dB the gain and directivity increased about 3 dB which indicates the duplication in dB.

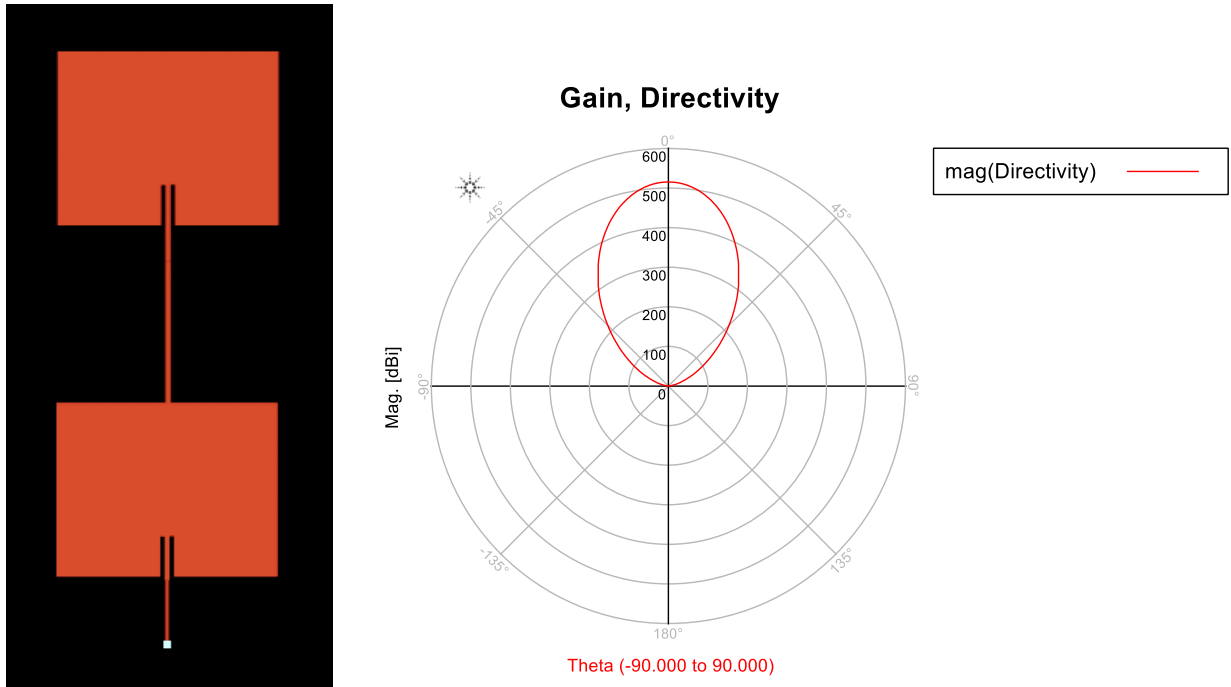


Figure 4.21 Two elements array L-band antenna

The simulation was done with the same parameters as in the previous simulation. Figure 4.23 presents the overall radiation pattern when the capacitance of the varactors is about 0.001 pf. We note from the figure that the directivity is doubled if we compare it with the result in Figure 4.17. In Figure 4.24, the radiation pattern is directed to theta equal to zero i.e. normal to the array surface by changing the capacitance of the varactors to 1.5 pf. As we can see, we are able to have any scanning angle with an acceptable gain by changing the varactors capacitance in the phase shifters between 0.001-4.5 pf.

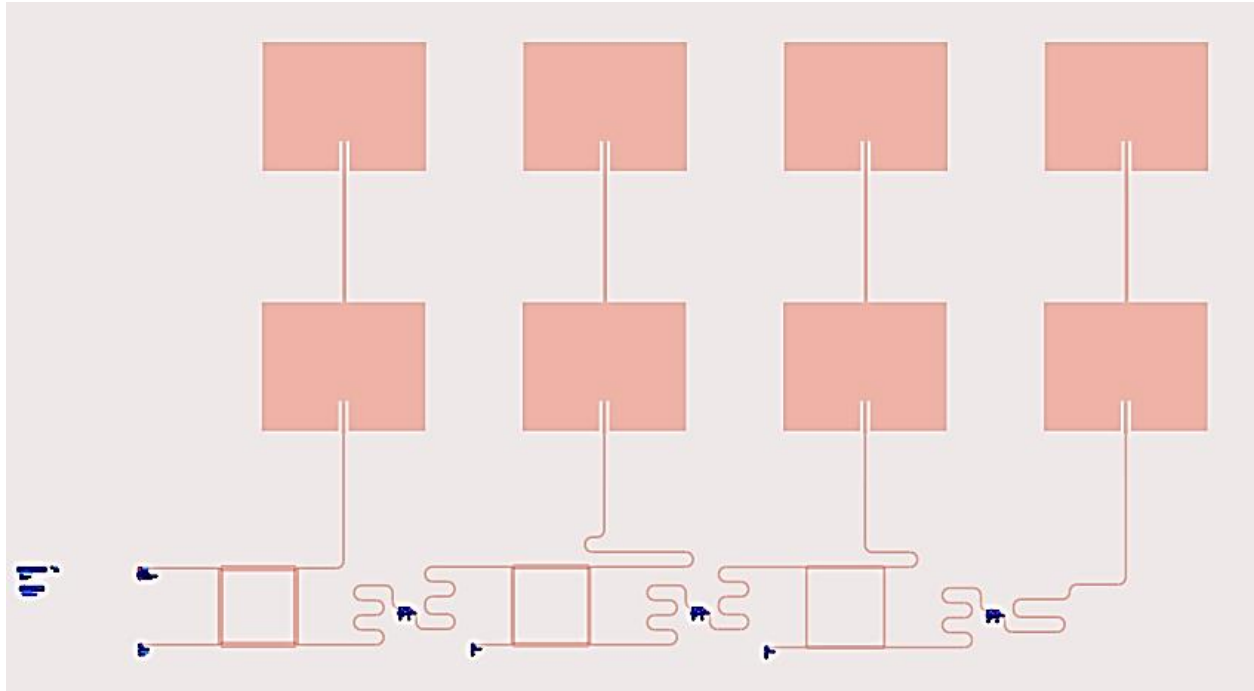


Figure 4.22 Beamforming circuit with L-band subarrays

In Figure 4.24 (b), the directivity and also the gain of the overall system decreased due to the decreasing in insertion loss of phase shifters when the capacitance increased above 4.5 pf. In general, the low gain at 4.5 pf is acceptable case because there is minimum side lobe effect.

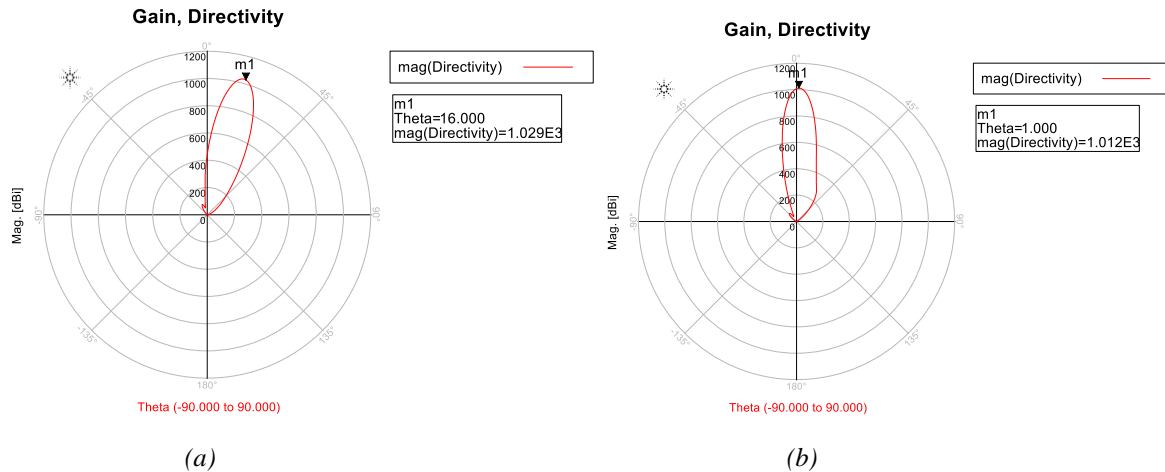


Figure 4.23 Radiation pattern of new phased array when (a) $C=0.001$ pf, (b) $C=1.5$ pf

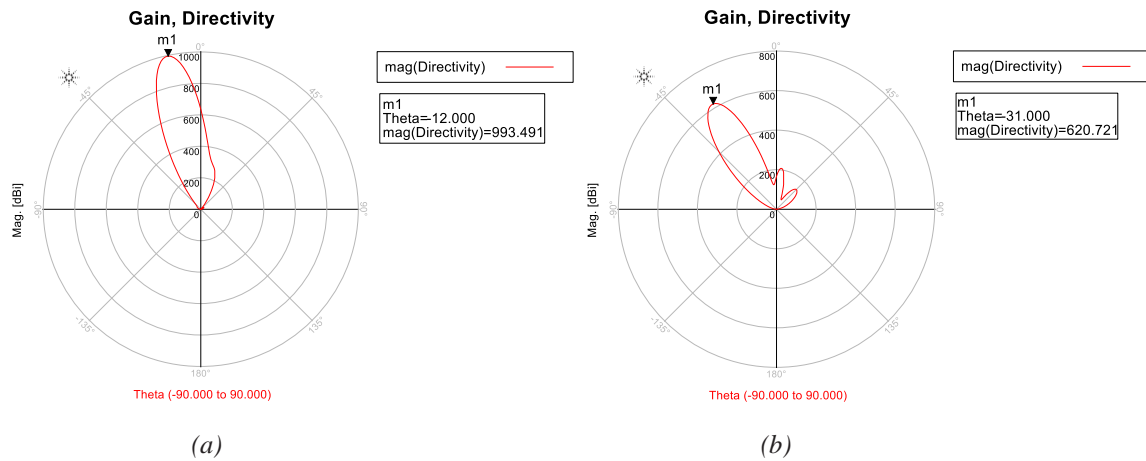


Figure 4.24 Radiation pattern of new phased array when (a) $C=3$ pf, (b) $C=4.5$

4.4.3 Design of Ku-band antenna

The main component in the overall design is the antenna which will be used in order to receive the satellite channels, which is designed in Ku-band. The dimensions of this antenna are shown in Figure 4.25. The slots that appear in the sides of antenna are used to increase the gain.

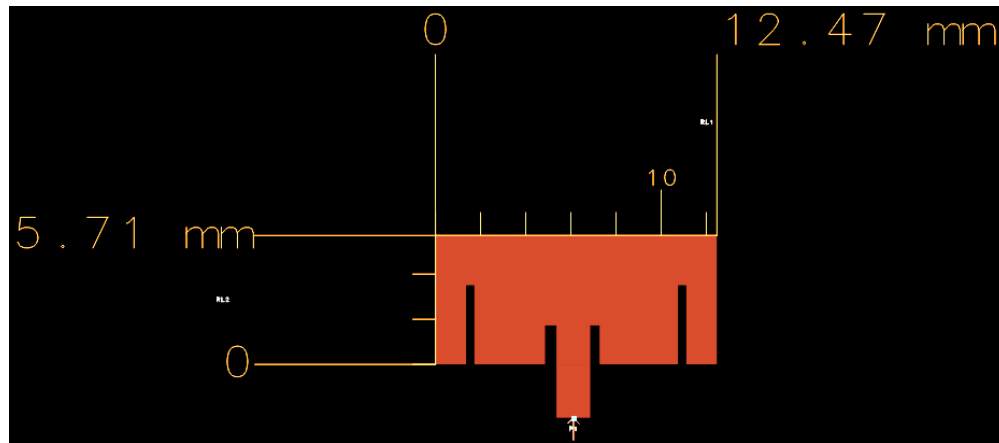


Figure 4.25 Ku-band Antenna dimensions

The 2D Radiation pattern of the antenna is shown in Figure 4.26. It is noticed that the gain is about 6 dB at theta equal zero and directivity is about 8 dB.

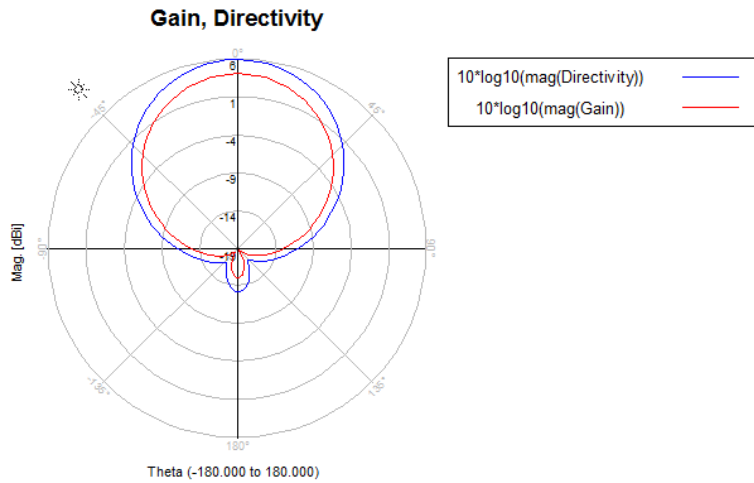


Figure 4.26 2D Radiation Pattern of Ku-band antenna

Figure 4.27 shown the return loss when the antenna is matched to 50 ohm. The minimum value of the antenna return loss is about -15.8 dB and the -10 dB bandwidth of the antenna is approximately 400 MHz at the center frequency of 12.1 GHz.

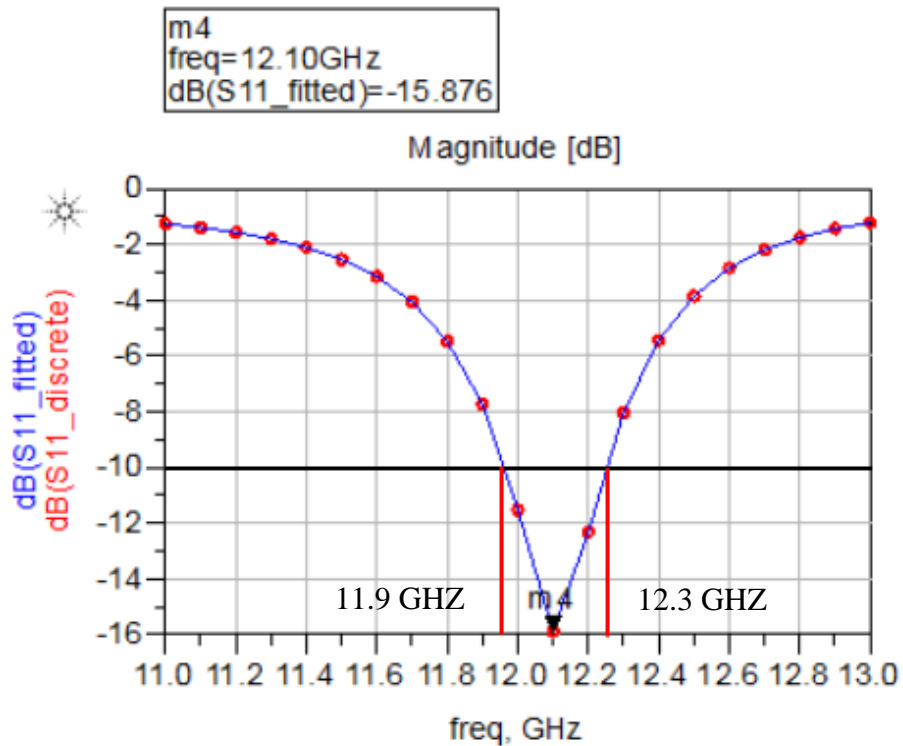


Figure 4.27 Ku-band Antenna return loss

Next section, an array of four elements will be designed for increasing the gain.

4.5 4-Element Array Design

An array of antenna elements is designed in order to increase the gain and directivity of antenna and also to decrease the beamwidth of the radiation pattern for concerning the power in a specific angle. Figure 4.28 shows the dimensions of array.

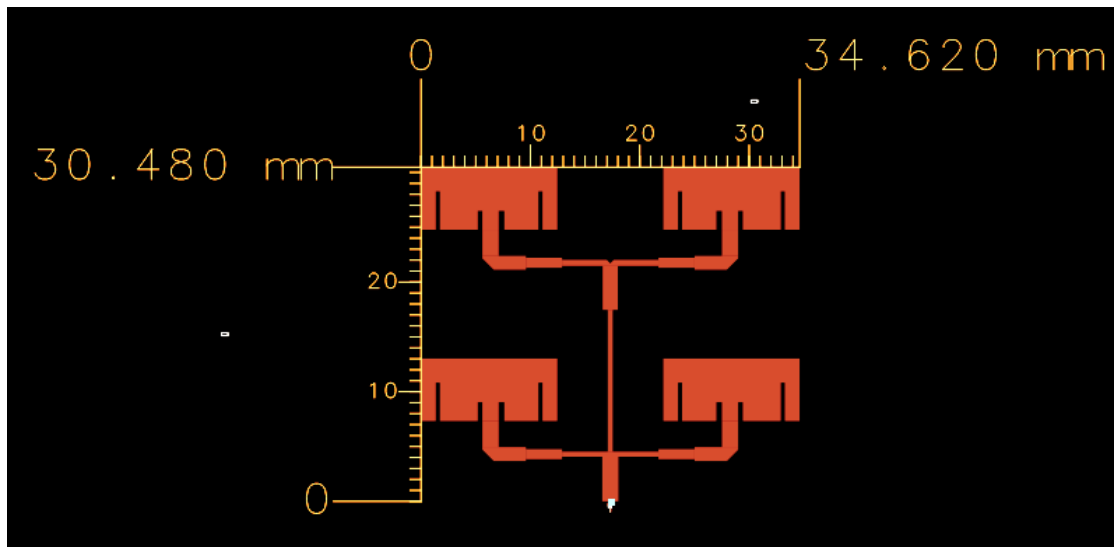


Figure 4.28 Ku-band Array antenna dimensions

In order to have higher gain and maximum value of radiation pattern at the center of array, we have to design a feeding network which has to distribute the power from the source to the array elements with same amplitude and phase. The 2D Radiation pattern of the array is shown in Figure 4.29. As we can see from the figure that the gain is about 11.7 dB at theta equal zero and directivity is about 13.8 dB.

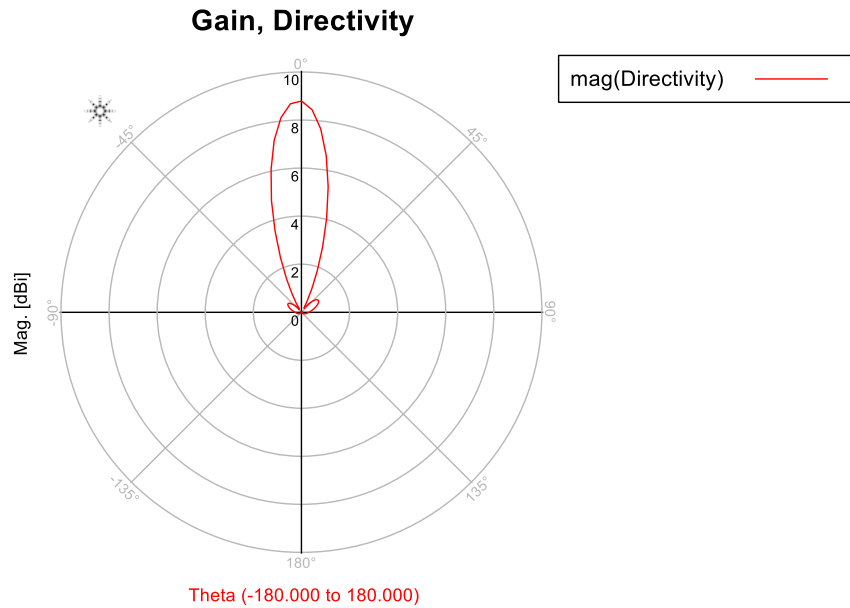


Figure 4.29 2D radiation pattern of Ku-band array

The return loss of the array when it is matched to 50 ohm is shown in Figure 4.30. The minimum value of the antenna return loss is about -35 dB and the -10 dB bandwidth of the antenna is approximately 0.5 GHz at the center frequency of 12 GHz.

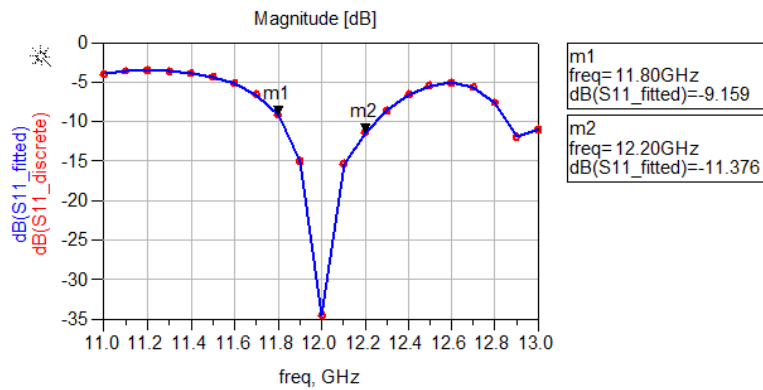


Figure 4.30 Array Antenna return loss (S11)

4.6 Simulation of the whole system

The steering in Ku-band requires a mixer with local oscillator frequency equal to 10.6 GHz. The feeding network of LO has to distribute the LO signal with same amplitude and with initial phase progression equal -14.5 to cancel the phase in IF-port. The 4-elements array antenna that discussed before will be the elements of the overall array so we call all it sub-array. The overall system with

steering circuit is shown in Figure 4.31. It is expected to have a steering angle equal to that found in the L-band because the phase shift does not change as we can see from the equations in the beginning of this chapter.

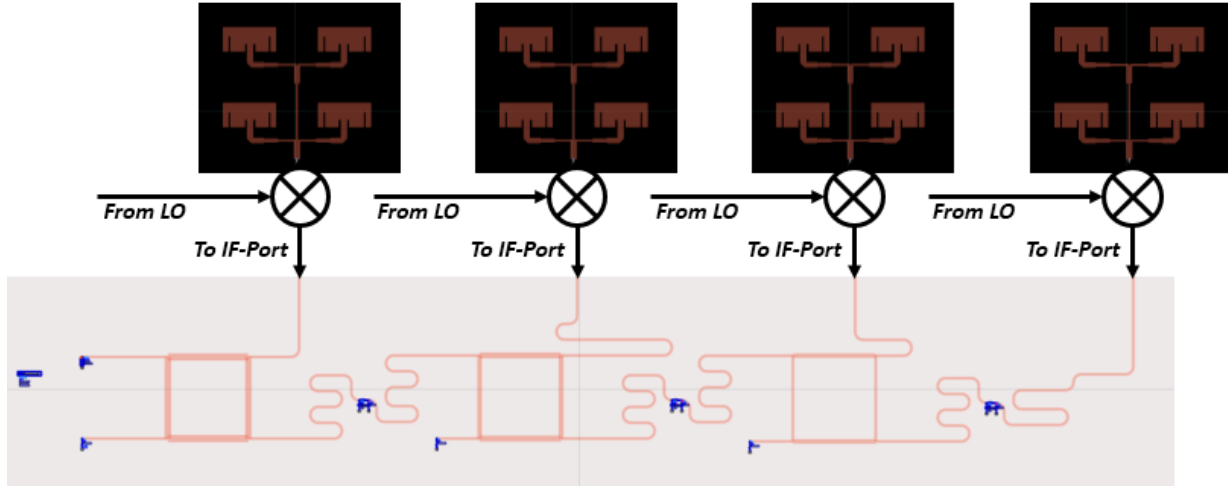


Figure 4.31 Ku-band steering system

4.7 Conclusion

In this chapter, beamforming circuit using hybrid couplers was presented with L-band antennas. The steering angle obtained from the simulation done in ADS 2014 is about 50 degree. Two elements array antenna in L-band was designed to increase the overall gain of the steering system. In order to perform the steering in Ku-band we also designed an array of Ku-band antennas. The overall system in Ku-band need a mixer in order to connect the L-band steering circuit with Ku-band radiating antennas.

5. Conclusion and future work

In conclusion, this thesis presents a developed technique to design phased array antenna with reduced complexity of the overall system. The phased array feeding network is capable of reducing the complexity of phased array antenna by achieving phase shifting and power dividing within a single network. The phase shifting is done at the IF stage and the feeding network is series fed and designed at center frequency of 1.7 GHz and used hybrid couplers in order to distribute the signal to its ports with the same power with the ability to change the signal phase upon the required scan angle via three phase shifters. The phase shifters used in the design here consist of varactor diodes and when the bias voltage is changed from 0.6 VDC to 8.5 VDC the capacitance changes from 28 pF to 1 pF. To evaluate the steering ability of the designed structure, microstrip patch antennas have been designed at 1.7 GHz and added to the ports of the steering network. Each antenna is an inset-fed with gain of 2.02 dB and FBW of 5 %. The overall gain of the resulting array is 8 dB. The maximum steering angle range obtained from the simulation performed in ADS 2014 is about 50 degree with maximum gain variation about 1.3 dB. The overall system is designed at Ku-band at 12.2 GHz. Patch antennas have been designed at 12.2 GHz for satellite communications and the beam steering network designed at IF stage can be used to perform the steering. The Ku band single patch antenna has FBW of 3.5 % and gain of 6 dB. It designed with inset-feeding with two slots in the radiating element. The system still needs mixers with center frequency of 10.6 GHz to connect the L-band (1.7 GHz) steering circuit with Ku-band (12.2 GHz) radiating antennas and perform frequency conversion. The design of mixers is not in the scope of this thesis.

5.1 Performance Comparison

Table 5.1 summarizes the performance of the proposed phased array against other series-fed steerable arrays presented in the literature. The proposed antenna array achieves a wider electronic scan-angle range compared to many designs shown in Table 5.1. In [5], a wide scanning angle is obtained but with large variation in gain which is 13 dB. In the presented work, the gain variation is only 1.3 dB while obtaining a scanning angle of 50 degrees.

Table 5.1 Comparison between the series-fed phased array presented in this chapter and the published series-fed phased arrays

	[63]	[64, 65]	[66]	[67]	[68]	The Presented Phased Array
Number of antenna elements	4	5	30 leaky wave	4	4	4
Center frequency	2.45 GHz	5.8 GHz	3.33 GHz	2 GHz	2.4 GHz	1.7 GHz
Scan Range	30 degrees	22 degrees	60 degrees	20 degrees	49 degrees	50 degrees
Number of tuning voltages	6	1	1	4	3	1
Gain variation within scan range	NA	0.4 dB	13 dB	1.8 dB	1.5 dB	1.3 dB

5.2 Future Work

The important parameter of any phased array system is its scanning angle and its gain. So increasing the scanning angle by changing the reference port is a future contribution. Increasing the scanning angle may be done also by increasing the number of array element that will increase the gain of overall antenna which is a good contribution of the system. The digital beamforming can be utilized using FPGA controller which is available more than any microwave MMIC in our region so we can using it in any steering system in the future work. Furthermore, the designed circuit will be fabricated and tested to verify the simulation results.

Appendix A

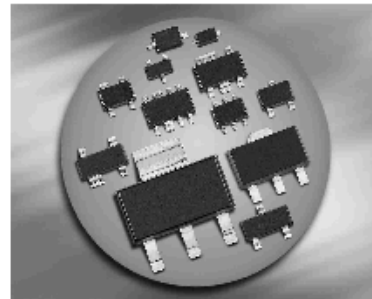
BB833 Varactor



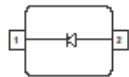
BB833...

Silicon Tuning Diodes

- Extended frequency range up to 2.5 GHz; special design for use in TV-sat tuners
- High capacitance ratio
- Pb-free (RoHS compliant) package



BB833



Type	Package	Configuration	L_S (nH)	Marking
BB833	SOD323	single	1.8	white X

Maximum Ratings at $T_A = 25^\circ\text{C}$, unless otherwise specified

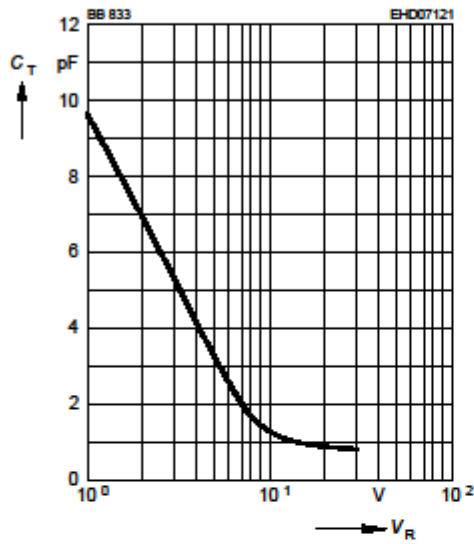
Parameter	Symbol	Value	Unit
Diode reverse voltage	V_R	30	V
Peak reverse voltage- $R \geq 5\text{k}\Omega$	V_{RM}	35	
Forward current	I_F	20	mA
Operating temperature range	T_{op}	-55 ... 150	$^\circ\text{C}$
Storage temperature	T_{stg}	-55 ... 150	

Electrical Characteristics at $T_A = 25^\circ\text{C}$, unless otherwise specified

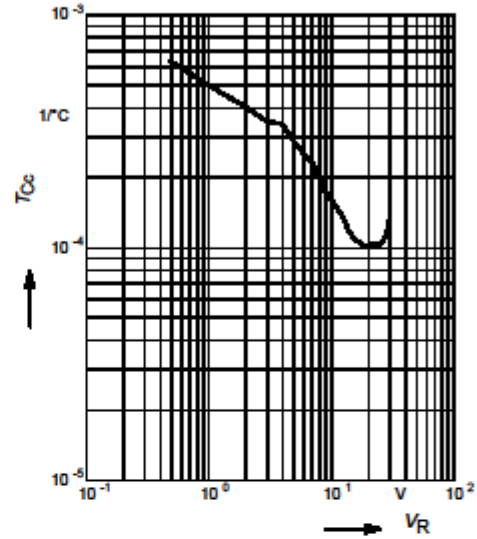
Parameter	Symbol	Values			Unit
		min.	typ.	max.	
DC Characteristics					
Reverse current	I_R				nA
$V_R = 30\text{ V}$		-	-	20	
$V_R = 30\text{ V}, T_A = 85^\circ\text{C}$		-	-	500	
AC Characteristics					
Diode capacitance	C_T				pF
$V_R = 1\text{ V}, f = 1\text{ MHz}$		8.5	9.3	10	
$V_R = 28\text{ V}, f = 1\text{ MHz}$		0.6	0.75	0.9	
Capacitance ratio	C_{T1}/C_{T28}	11	12.4	-	
$V_R = 1\text{ V}, V_R = 28\text{ V}, f = 1\text{ MHz}$					
Capacitance matching ¹⁾	$\Delta C_T/C_T$	-	-	3	%
$V_R = 1\text{ V}, V_R = 28\text{ V}, f = 1\text{ MHz}$					
Series resistance	r_S	-	1.8	-	Ω
$V_R = 1\text{ V}, f = 470\text{ MHz}$					

¹⁾For details please refer to Application Note 047.

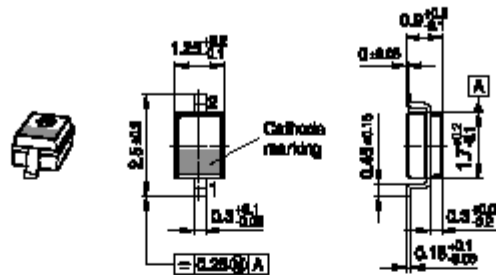
Diode capacitance $C_T = f(V_R)$
 $f = 1\text{MHz}$



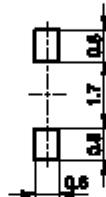
Temperature coefficient of the diode capacitance $T_{Cc} = f(V_R)$



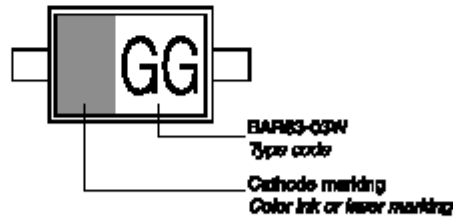
Package Outline



Foot Print

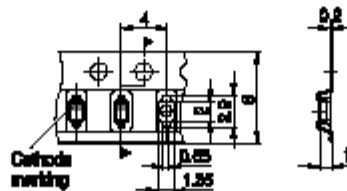


Marking Layout (Example)



Standard Packing

Reel ø180 mm = 3.000 Pieces/Reel
 Reel ø330 mm = 10.000 Pieces/Reel



Edition 2009-11-16

Published by
Infineon Technologies AG
81726 Munich, Germany

© 2009 Infineon Technologies AG
All Rights Reserved.

Legal Disclaimer

The information given in this document shall in no event be regarded as a guarantee of conditions or characteristics. With respect to any examples or hints given herein, any typical values stated herein and/or any information regarding the application of the device, Infineon Technologies hereby disclaims any and all warranties and liabilities of any kind, including without limitation, warranties of non-infringement of intellectual property rights of any third party.

Information

For further information on technology, delivery terms and conditions and prices, please contact the nearest Infineon Technologies Office (www.infineon.com).

Warnings

Due to technical requirements, components may contain dangerous substances. For information on the types in question, please contact the nearest Infineon Technologies Office.

Infineon Technologies components may be used in life-support devices or systems only with the express written approval of Infineon Technologies, if a failure of such components can reasonably be expected to cause the failure of that life-support device or system or to affect the safety or effectiveness of that device or system. Life support devices or systems are intended to be implanted in the human body or to support and/or maintain and sustain and/or protect human life. If they fail, it is reasonable to assume that the health of the user or other persons may be endangered.

6. References

- [1] S. W. L., Antenna theory and design.
- [2] D. Ehyai, "Novel Approaches to the Design of Phased Array Antennas," University of Michigan, 2011.
- [3] R. C. HANSEN, Phased Array Antennas.
- [4] C. A. Balanis, ANTENNA THEORY, A JOHN WILEY & SONS, INC., 2005.
- [5] A. T. team, "Advanced Design System," Adilent EEsof EDA.
- [6] D. Roddy, Satellite Communication.
- [7] R. Baggen and S. Vaccaro, "A SATCOM PHASED ARRAY IN KU-BAND," 2012.
- [8] M. M. Bilgiç, K. Yeğın, T. Türkkın and M. Sengiz, "Design of a Low-Profile Ku Band Phased Array Antenna for Mobile Platforms".
- [9] G. Zomchek and S. Laxpati , "S-Band Phased Patch Array Design for Satellite Applications," University of Illinois at Chicago.
- [10] K. Saito, M. Takahashi and K. Ito, "Field Measurement on Simple Vehicle-Mounted Antenna System Using a Geostationary Satellite".
- [11] Gregoire, D.J, Colburn, P. J.S, A. Quarfoth and R. Sievenpiper, "A low profile electronically-steerable artificial-impedance-surface antenna".
- [12] S. d. Vaccaro, D.Sanchez, R.T. and R. Baggen, "Low cost phased array for mobile ku-band satellite terminal".
- [13] L. Zhiqiang, M. Yao and X. Shen, "Sidelobe Reduction of the Low Profile Phased Array Antenna for Satellite Communication on-the-Move".
- [14] Y. Huang and K. Boyle, ANTENNAS, A John Wiley and Sons, Ltd, 2008.
- [15] J. D. Kraus, ANTENNAS, 1988.
- [16] M. N. O. SADIKU, Elements of Electromagnetics, NEW YORK: Oxford University Press, 2007.
- [17] S. J. Orfanidis, Electromagnetic Waves and Antenna, Rutgers University, 2014.

- [18] R. Rodrigo, *Fundamental Parameters of Antennas*, 2010.
- [19] R. S. Elliott, *ANTENNA THEORY AND DESIGN*, A JOHN WILEY & SONS, INC., 2003.
- [20] J. HUANG, *Microstrip Antennas: Analysis, Design, and Application*.
- [21] I. J. Bahl and P. Bhartia, *Microstrip Antennas*, Artech House, Norwood, MA, 1980.
- [22] J. R. James and P. S. Hall, *Handbook of Microstrip Antennas*, Peter Peregrinus Ltd., London, 1989.
- [23] L. Murphy, "SeaSAT and SIR-A microstrip antennas," *Proceedings of the Workshop on Printed*, p. 18, 1979.
- [24] J. Huang, M. Lou, B. C. Lopez and E. Gama, "Foldable frame-supported thin-membrane array," *Proceedings of the International Symposium on Antennas and Propagation (ISAP)*, p. 213–216, 2000,.
- [25] S. A. Long and M. D. Walton, "A dual-frequency stacked circular disc antenna," *Digest of the International Symposium of the Antennas Propagation Society*, p. 260–263, 1978.
- [26] P. S. Hall, "Probe compensation in thick microstrip patches," *Electron. Lett*, vol. 23, p. 606–607, 1987.
- [27] J. Huang, "Stripline feed for a microstrip array of patch elements with teardrop shaped probes," *U.S. Patent*, 1990.
- [28] R. F. Thomas and J. Huang, "Ultra-wideband UHF microstrip array for GeoSAR applications," *IEEE Antennas and Propagation Society International Symposium*, p. 2096–2099, 1998.
- [29] J. Huang and D. M. Pozar, "Chapter 3," in *Advances in Microstrip and Printed Antennas*, John Wiley & Sons, Hoboken, 1997.
- [30] P. Bhartia, K. V. S. Rao and R. S. Tomar, "Millimeter-Wave Microstrip and Printed Circuit," Boston, 1991.
- [31] D. M. Pozar, "Microstrip antenna aperture-coupled to a microstripline," *Electron. Lett.*, vol. 21, p. 49–50, 1985.
- [32] D. H. Schaubert, D. M. Pozar and A. Adrian, "Effect of Microstrip Antenna Substrate," *IEEE Trans. Antennas Propagat.*, Vols. AP-37, p. 677–682, 1989.

- [33] C. A. Balanis, *Advanced Engineering Electromagnetics*, New York: John Wiley & Sons, 1989.
- [34] E. O. Hammerstad, "Equations for Microstrip Circuit Design," in *Proc. Fifth European Microwave*, 1975.
- [35] I. J. B. a. P. Bhartia, *Microstrip Antennas*, Artech House: Dedham, MA, 1980.
- [36] W. F. Richards, "Microstrip Antennas," in *Antenna Handbook: Theory, Applications*, New York, Van Nostrand Reinhold Co, 1988.
- [37] G. V. TSOULOS and C. G. CHRISTODOULOU, *Arrays and Smart Antennas*, Canada: A JOHN WILEY & SONS, 2008.
- [38] C. A. Balanis, *Antenna Theory: Analysis and Design*, Hoboken: John Wiley & Sons, 1997.
- [39] M. S. Bartlett, *An Introduction to Stochastic Process*, Cambridge: Cambridge University Press, 1956.
- [40] S. P. Applebaum, "Adaptive arrays," *IEEE Trans. Antennas Propag.*, vol. 24, no. 5, p. 585–598, 1976.
- [41] B. Widrow, P. E. Manteufel, L. J. Griffiths and B. B. Goode, "Adaptive antenna systems," *IEEE Proc.*, vol. 55, no. 12, p. 2143–2159, 1967.
- [42] R. M. a. T. Miller, *Introduction to Adaptive Arrays*, Hoboken: John Wiley & Sons, 1980.
- [43] L. C. Godara, "Application of antenna arrays to mobile communications," *Proc. IEEE*, vol. 85, no. 8, p. 1195–1245, 1997.
- [44] J. Butler and R. Lowe, "Beamforming matrix simplifies design of electronically scanned antennas," *Electron. Design*, 1961.
- [45] J. P. Shelton and K. S. Kelleher, "Multiple beams from linear arrays," *IRE Trans. Antennas*, 1961.
- [46] J. Litva and T. Lo, *Digital Beamforming in Wireless Communications*, London: Artech House, 1996.
- [47] R. G. Pridham and R. A. Mucci, "Digital interpolation beamforming for low-pass and bandpass," *Proc. IEEE*, vol. 67, no. 5, p. 904–919, 1979.
- [48] S. Anderson, M. Millnert and M. Viberg, "An adaptive array for mobile communication," *IEEE Trans. Vehicular Technol.*, vol. 40, no. 2, p. 230–236, 1991.

- [49] H. J. Visser, *Array and Phased Array Antenna Basics*, John Wiley & Sons, 2005.
- [50] R. Johnson, *Antenna Engineering Handbook*, third edition, New York: McGraw-Hill, 1993.
- [51] M. I. Skolnik, *Introduction to Radar Systems*, second edition, New York: McGraw-Hill, 1993.
- [52] Y. Lo and S. Lee, *Antenna Handbook, Applications*, Kluwer Academic, 1993.
- [53] R. C. Hansen, *Phased array antennas*, Wiley-Interscience, 2009.
- [54] R. C. Johnson and H. Jasik, *Antenna engineering handbook*, 1984.
- [55] R. J. M. a. I. Books, *Phased array antenna handbook*, Artech House, 2005.
- [56] D. M. Pozar and D. H. Schaubert, "Comparison of three series fed microstrip," *Antennas and Propagation Society International Symposium*, vol. 2, pp. 728-731, 1993.
- [57] E. Cohen, C. Jakobson, S. Ravid and D. Ritter, "A bidirectional TX/RX four element phased-array at 60GHz with RF-IF conversion block in 90nm CMOS process," *Radio Frequency Integrated Circuits Symposium*, pp. 207-210, 2009.
- [58] W. Chao-Shiun, H. Juin-Wei, C. Kun-Da and W. Chorng-Kuang, "A 60-GHz Phased Array Receiver Front-End in 0.13-um CMOS Technology," *Circuits and Systems I: Regular Papers, IEEE Transactions on*, vol. 56, pp. 2341-2352, 2009.
- [59] K. Scheir, S. Bronckers, J. Borremans, P. Wambacq and Y. Rolain, "A 52 GHz Phased-Array Receiver Front-End in 90 nm Digital CMOS," *Solid-State Circuits IEEE Journal*, vol. 43, pp. 2651-2659, 2008.
- [60] A. Natarajan, A. Komijani and A. Hajimiri, "A fully integrated 24-GHz phased phasedarray," *Solid-State Circuits, IEEE Journal of*, vol. 40, pp. 2502-2514, 2005.
- [61] D. Ehyaie and A. Mortazawi, "A 24 GHz modular phased array based on extended resonance technique," *Phased Array Systems and Technology (ARRAY), 2010 IEEE International Symposium*, pp. 814-818, 2010.
- [62] D. Ehyaie and A. Mortazawi, "A 24-GHz Modular Transmit Phased Array," *Microwave Theory and Techniques, IEEE Transactions on*, vol. 59, pp. 1665-1672, 2011.

- [63] M. Tsuji, T. Nishikawa, K. Wakino and T. Kitazawa, "Bi-directionally fed phased-array antenna downsized with variable impedance phase shifter for ISM band," *Microwave Theory and Techniques, IEEE Transactions on*, vol. 54, pp. 2962-2969, 2006.
- [64] E. Ojefors, C. Shi, K. From, I. Skarin, P. Hallbjorner and A. Rydberg, "Electrically Steerable Single-Layer Microstrip Traveling Wave Antenna With Varactor Diode Based Phase Shifters," *Antennas and Propagation, IEEE Transactions on*, vol. 55, pp. 2451-2460, 2007.
- [65] C. Shi, E. Ojefors, P. Hallbjorner and A. Rydberg, "Compact reflective microstrip phase shifter for traveling wave antenna applications," *Microwave and Wireless Components Letters, IEEE*, vol. 16, pp. 431-433, 2006.
- [66] L. Sungjoon, C. Caloz and T. Itoh, "Metamaterial-based electronically controlled transmission-line structure as a novel leaky-wave antenna with tunable radiation angle and beamwidth," *Microwave Theory and Techniques, IEEE Transactions on*, vol. 52, pp. 2678-2690, 2004.
- [67] A. Tombak and A. Mortazawi, "A novel low-cost beam-steering technique based on the extended-resonance power-dividing method," *Microwave Theory and Techniques, IEEE Transactions on*, vol. 52, pp. 664-670, 2004.
- [68] M. A. Y. Abdalla, K. Phang and G. V. Eleftheriades, "A Planar Electronically Steerable Patch Array Using Tunable PRI/NRI Phase Shifters," *Microwave Theory and Techniques, IEEE Transactions on*, vol. 57, pp. 531-541, 2009.
- [69] P. K. Mathew, S. M. G. Raj and U. P. A.J, "Compact Multiband Antenna for Wireless and Satellite Communication".
- [70] J. D. Kraus, *Antennas*, New York: McGraw-Hill, 1988.
- [71] K. F. Sander and G. A. L. Reed, *Transmission and Propagation of Electromagnetic Waves*, Cambridge: Cambridge University Press, 1986.
- [72] W. L. Stutzman and G. A. Thiele, *Antenna Theory and Design*, Hoboken: John Wiley & Sons, 1981.